DYNAMIC DEVICES
A PRIMER ON PICKUPS AND KICKERS

D.A. Goldberg and G.R. Lambertson
Lawrence Berkeley Laboratory, Berkeley California 94720

TABLE OF CONTENTS

C. PROPERTIES OF SPECIFIC DEVICES

DYNAMIC DEVICES
A PRIMER ON PICKUPS AND KICKERS

D.A. Goldberg and G.R. Lambertson
Lawrence Berkeley Laboratory, Berkeley California 94720

A. INTRODUCTION

A charged-particle beam generates electromagnetic fields which in turn interact with the beam's surroundings. These interactions can produce fields which act back on the beam itself, or, if the "surroundings" are of suitably designed form (e.g., sensing electrodes with electrical connection to the "outside world"), can provide information on various properties of the beam; such electrodes are generally known as *pickups*. Similarly, charged-particle beams respond to the presence of externally imposed electromagnetic fields; devices used to generate such fields are generally known as *kickers*. As we shall show, the behavior of an electrode system when it functions as a pickup is intimately related to its behavior as a kicker.

A number of papers on pickup behavior have appeared in recent years [1-5] in most of which the primary emphasis has been on beam instrumentation; there have also been several workshops on the subject [6,7]. There have been several papers which have treated both pickup and kicker behavior of a particular electrode system [8.9], but this has been done in the context of discussing a specialized application, such as a stochastic cooling system.

The approach in the present paper is similar to that of earlier works by one of the authors [10,11], which is to provide a unified treatment of pickup and kicker behavior, and, it is hoped, to give the reader an understanding which is both general and fundamental enough to make the above references easily accessible to him. The paper is basically an expanded version of Ref. 10. As implied by the revised title, we have done the re-writing with the non-expert in mind. We have made the introduction both lengthier and more detailed, and done the same with much of the explanatory material and discussion.

We begin with an overview which, in addition to providing a general background for the succeeding material, will also serve to introduce some of the terminology and notation. Because most electrodes can serve as either pickup or kicker, in the discussion which follows we will frequently refer interchangeably to the behavior of such a system in terms of its behavior as either pickup or kicker, with the understanding that words such as "detect" or "respond", as applied to the pickup be changed to "influence" or "affect" as applied to the kicker.

It is conventional usage to refer to electrode systems which respond only to the total beam current as *longitudinal* devices, because their response turns out to be sensitive only to those properties of the beam which are associated with its longitudinal motion (e.g., revolution frequency, longitudinal emittance, pulse length). Those systems which respond to the product of the current and the transverse displacement are known as *transverse* devices, because they are sensitive properties of the beam's transverse motion (e.g. betatron tune, transverse emittance). As with the case of the pickup/kicker duality, we shall see that the longitudinal and transverse responses of an electrode system are intimately related.

Schematically we can represent a longitudinal or a transverse kicker as a "black box" as shown in Figs. 1a and 1b:

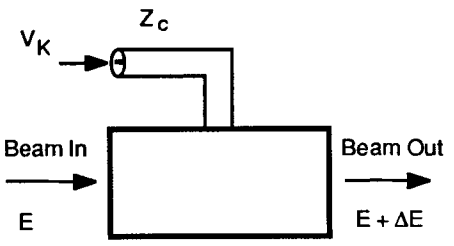

Fig. 1a Schematic Model of Longitudinal Kicker

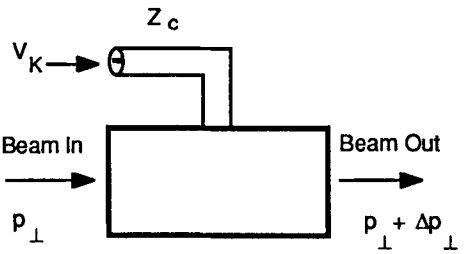

Fig. 2b Schematic Model of Transverse Kicker

A (time-varying) voltage is injected onto an electrode structure internal to the black box as a result of a voltage V_K being impressed on an input signal cable of characteristic impedance Z_c. The resulting electrode voltage produces a change in either the energy (E) or transverse momentum ($p_\perp$) of the particles in the beam passing through the structure.

A word on some of the conventions to be employed may be appropriate. As per the above figures, we will use the parallel symbol (∥) to denote quantities related to longitudinal motion; the perpendicularity symbol (⊥), transverse motion. We could equally well have used $p_\parallel$ as the characteristic of longitudinal motion but the energy turns out to be a more convenient parameter. It is frequently convenient to express the change in beam energy in terms of an equivalent beam voltage $V \equiv \Delta E/e$, where e is the electron charge; the beam voltage has the same numerical value as the change in beam energy expressed in electron volts. One can define a corresponding transverse beam voltage as $\Delta p_\perp \beta c/e$, where $\beta c = v$, the (longitudinal) beam velocity; in many accelerators $v \approx c$, so that $\beta \approx 1$. (Those wishing either a brief review of, or a crash course in elementary relativistic dynamics are referred to Appendix 1.)

We can employ a schematic representation for pickups similar to that used for kickers: A beam of particles passing through the black box causes a signal to appear at the end of a signal cable which is (possibly indirectly) connected to an internal beam-sensing electrode structure. For a longitudinal pickup, the output signal is proportional to the beam current; for a transverse pickup, it is proportional to the product of the beam current and the beam's transverse displacement, i.e. to the dipole moment of the beam.

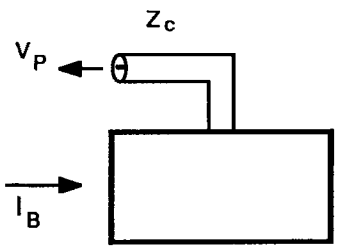

Fig. 2a Schematic Model of Longitudinal Pickup

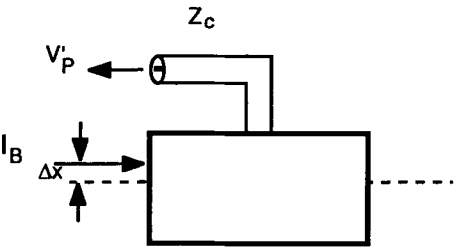

Fig. 2b Schematic Model of Transverse Pickup

For those with little background in the subject, an overly simplified example may serve not only to illustrate the ideas we have been discussing, but to provide a physical example to consider while we introduce some general theorems in the next section. Let us consider a set of electrodes consisting of a pair of parallel plates on opposite sides (say, top and bottom) of the beam,which are sufficiently wide that we can ignore any effects due to the lateral position of the beam, and let us consider its interaction with a single, short beam pulse.

Considering the behavior of the electrodes acting as a pickup, it should be plausible, if not obvious, that the signal obtained by adding the voltages on the upper and lower plates is proportional to the total charge of the beam pulse (i.e. the current), and to first order is independent of the vertical position of the beam. On the other hand, the signal obtained by *subtracting* the voltages on the upper and lower plates is to first order proportional to the vertical position of the beam. In other words, the same electrode system can be used to sense both the longitudinal and transverse properties of the beam.

In like fashion, were we to apply an external signal to the two plates, we would be able to be able to influence the beam's motion: If we excited the two plates with voltages which were equal in both magnitude and sign, we could give the beam a longitudinal kick; if the voltages were equal in magnitude but *opposite* in sign, the beam would receive a *transverse* kick. Hence the same electrode system may function as either a pickup or a kicker.

We alluded earlier to the fact that kicker voltages were time-varying. In fact, in our example of the parallel-plate electrodes, we can see that placing a dc voltage on the plates will produce no net change in the longitudinal motion of the beam: If the beam underwent an acceleration when entering the plates, it would experience an equal and opposite deceleration when leaving them; a time-varying field is necessary for a net longitudinal kick. (In contrast, a dc voltage across the plates *would* result in a *transverse* beam deflection.)

In treating the time-dependent variation of kicker voltages, we will make use of the fact that such voltages can be expressed as a superposition of sinusoidal waves and will henceforth assume that, unless specified otherwise, all time dependent quantities such as V_K are sinusoids; this approach should be recognizable to electrical engineers as a *frequency-domain* analysis. Since beams in particle accelerators are also time-dependent, a similar approach will be used for the treatment of pickups. For bunched beams, it is probably not surprising that the frequencies of interest will be those associated with both the bunch length and the bunch-to-bunch separation (the reciprocal of the separation period as well as its higher harmonics); for a circular machine, harmonics associated with the revolution period (a subharmonic of the bunch-separation frequency) will also be of interest. What is perhaps less obvious is that these latter frequencies are also of interest in the case of signals from an *unbunched* beam in a circular machine, the so-called Schottky signals, which will be described later.

The main body of the paper will be divided into two sections. The first of these deals with basic principles and theorems, including such topics as figures of merit for pickups and kickers, the frequency spectra of charged-particle beams, and a brief discussion of beam impedance. The second section will illustrate the application of these ideas by analyzing the performance of a variety of electrode systems. We have included two appendices, one on relativistic particle dynamics (to which we have already made reference) and a second on integrals involving time-varying fields. Including this material in the form of appendices avoided interruption of the flow of the arguments, and, hopefully, irritation of the more expert reader. References to this material appear at the relevant places; however we leave it up to the individual reader to decide on the appropriate times to consult it.

B. BASIC PRINCIPLES

1. Some General Theorems

As we have already mentioned, an electrode system which can be used as a kicker can also function as a pickup, although as a practical matter not every electrode system may find application in both roles. The first two theorems in this section, dealing with reciprocity, demonstrate the relationships between the behavior in both roles. The third theorem demonstrates the relationship between the longitudinal and transverse effects of an electrode system. The results are derived in terms of kicker performance; by virtue of reciprocity, the results are equally applicable to pickup behavior.

a. Relation Between Kicker and Pickup Performance

In analyzing the behavior of an electrode system, it frequently proves easier to calculate its behavior as a kicker, i.e. the response of the beam when the structure is powered externally, than it is its performance as a pickup, where one must solve a boundary-value problem with the beam current as a source term. This is particularly true when, in the case of the kicker, the fields due to the presence of the beam are negligible compared to the externally applied fields. In any case, one practical consequence of these theorems is that one need calculate the device's behavior in only one of its modes of operation.

i. Lorentz Reciprocity Theorem The basic form of that theorem [12] states that if we have a volume V bounded by surface S, and we consider two independent modes of electromagnetic excitation (whose fields, for reasons which may already be apparent to the reader, we denote by subscripts K and B), with which are associated source currents $\mathbf{J_K}$ and $\mathbf{J_B}$, then if the fields and current flows are expressed as complex phasors with time dependence $e^{j\omega t}$ (i.e., using the frequency-domain analysis referred to earlier) we have the relation

$$\int_S \left(\mathbf{E_K}\times\mathbf{H_B}-\mathbf{E_B}\times\mathbf{H_K}\right)\cdot\mathbf{dS}=\int_{vol}\left(\mathbf{E_B}\cdot\mathbf{J_K}-\mathbf{E_K}\cdot\mathbf{J_B}\right)d\,vol\ . \tag{1.1}$$

The boundary which defines the surface and volume integrals in Eq. 1.1 is usually chosen to include not only the volume in which the fields are present, but the surrounding conducting surfaces as well.

To apply this somewhat abstract result to the case of the pickup/kicker problem, let us consider the device shown schematically in Fig. 3. An assembly containing some sort of electrode structure is located in an accelerator beam tube; signals to and from the electrode are transmitted to an external signal port, usually by a coaxial cable. The surface S surrounds the entire assembly, the only "penetrations" where fields may exist being the two beamline connections and the signal port.

Let subscript B (as in "beam") denote the fields present when the device functions as a pickup, where the fields generated by the presence of beam current I_B result in an outgoing signal, characterized by V_B, at the signal port. Let subscript K denote the fields and currents present when the device is excited as a kicker by the injection of an *ingoing* signal characterized by voltage V_K at that same port. The currents denoted by $\mathbf{J_B}$ include both the beam current I_B as well as any surface currents it may induce anywhere within the assem-

bly, including the signal cables. By way of contrast, the $\mathbf{J_K}$ include only those currents resulting from the presence of V_K. This is tantamount to asserting not only that the fields present during kicker operation are negligibly influenced by any beam currents present, but that such a current, if present, would be negligibly perturbed by such fields.

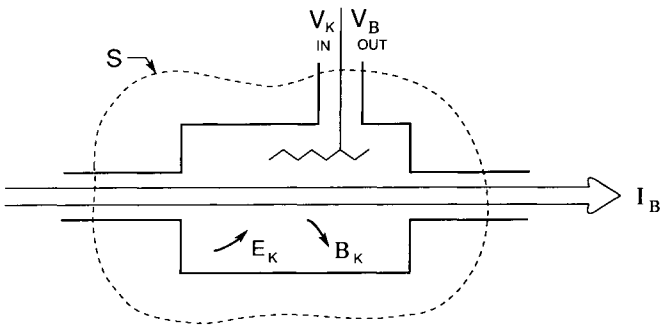

Fig. 3 Application of Reciprocity Theorem to Pickup/Kicker Geometry

For the surface S shown, the integral on the left hand side of Eq. 1.1 includes two types of surfaces at which fields may be present: entrance and exit beam apertures, and the signal port at the end of the input/output signal cable. In most practical cases, the kicker fields are strongly attenuated in the beam tubes; this is usually accomplished by operating at frequencies below the cutoff frequency of the beam tube, or through the use of damping materials. Hence we can usually simplify the calculation by defining S to intercept the beam tube at a sufficient distance that the contributions from the surface integrals over the beam tube apertures are negligible. For the signal port, if the input/output signals are TEM waves propagating in a cable of characteristic impedance Z_c, the signal voltage is simply the integral of the electric field between the inner and outer conductors; it is quite straightforward to show that each term in the surface integral contributes $V_K V_B / Z_c$.[1]

Turning to the volume terms on the right hand side of the equation, we note that since the fields and currents in resistive media are proportional, the sum of the terms involving currents in the walls and cables is zero. Therefore, since only for the pickup case are there source currents in free space, only the $\mathbf{E_K} \cdot \mathbf{J_B}$ term contributes to the integral. Applying the above considerations to Eq. 1.1 and transposing yields

$$V_B = -\frac{Z_c}{2V_K} \int_{vol} \mathbf{E}_K \cdot \mathbf{J_B}\, d\, vol\,. \tag{1.2}$$

Several features of Eq. 1.2 are worth pointing out explicitly. In evaluating the right hand side of Eq. 1.2, we must not only use the kicker fields that result when the device is excited by a kicker signal at frequency ω, but must use a sinusoidally varying current at that same frequency for $\mathbf{J_B}$ (see the discussion on frequency spectra of beams in Sect. 3). Another

[1] For those concerned with mathematical niceties, we could have chosen S so that the remaining surfaces, rather than being in field-free space, conformed with the conducting walls of the enclosure and the signal cables; provided these surfaces can be characterized by a surface wave impedance, the integrand would vanish on these, as well.

point to note is that the integral is to be taken at a fixed time. In general, the kicker field will have the form of a standing wave. However, since the beam current will exhibit a sinusoidal spatial variation, for devices longer than a half-wavelength, cancellation will begin to occur in the integral; hence, for other than travelling wave devices, the device length is typically less than one half a wavelength at the frequencies of interest. We will be using Eq. 1.2 in deriving relations among the various kicker/pickup relations, and will dispense with further comment until that point.

ii. Green's Reciprocation Theorem This related theorem [13] describes a reciprocity relation for electrostatic problems. However, it is also applicable to electromagnetic excitations, as we shall subsequently see. In its basic form, the theorem applies to a set of conductors (numbered from $i = 1$ to n) for which we consider two different modes of excitation, which we will again "arbitrarily" denote by the superscripts K and B. The theorem states that if in the first mode the conductors carry charge $Q^K{}_i$ and are at potentials $V^K{}_i$, and if in the second mode these quantities are $Q^B{}_i$ and are at potentials $V^B{}_i$,then we have the following reciprocal relation between the Q's and V's.

$$\sum_{i=1}^{n} Q_i^B \, V_i^K = \sum_{i=1}^{n} Q_i^K \, V_i^B \tag{1.3}$$

In addition to conductors, one can also include in the above summations point charges. In these cases the V_i represent the potential at the location of the ith charge due to all the *other* charges. It is not necessary that charges be at all such locations in both sums; however, if a charge is present at the ith location in one of the excitations, then the potential at that point for the second excitation must be included in the sum, whether or not a charge is present there in the latter excitation.

Consider the following problem, which frequently arises in the analysis of pickup behavior. Let us suppose that a charge Q_B contained in the beam passes among a group of one or more pickup electrodes; we wish to calculate the quantity g_i, the fraction of Q_B which is induced on the ith electrode. We can solve this problem using Eq. 1.3 by positing a second problem in which there is no charge at the former location of Q_B and we ground all of the conductors except the ith, which we maintain at potential $V^K{}_i$. If we make the assumption that the charges on the electrodes in the former mode are no different from what they would be if the electrodes were grounded (in this mode, this assumption applies to *all* the electrodes, including the ith one) then it is straightforward to show that

$$g_i \equiv \frac{Q_i^B}{Q^B} = -\frac{V^K}{V_i^K} \tag{1.4}$$

In other words, the fraction of the charge Q_B which appears on the ith electrode in the former mode is the same (but with opposite sign) as the ratio of the voltage at the point where Q_B was to the voltage on the ith electrode, with all other electrodes grounded. If we simply set $V^K{}_i = 1$, then $g_i = V^K$.

A few points are worth noting. Using our example of the simple parallel-plate electrodes as a model, the longitudinal signal, obtained by summing the voltages on the two plates, will turn out to be proportional to $g_1 + g_2$, whereas the transverse signal, obtained by subtracting them, will depend on $g_1 - g_2$. One can use superposition to simplify the calculation, by placing both plates at +1 for the former calculation, and using equal and opposite unit potentials for the latter.

b. The Panofsky Wenzel Theorem: Relation Between Longitudinal and Transverse Effects

Consider a particle of charge e and velocity $\mathbf{v}$ moving through a kicker along a path defined by its instantaneous velocity, $d\mathbf{s} = \mathbf{v}dt$. Its total momentum change in passing from point a to point b is given by

$$\Delta\mathbf{p} = e\int_{t_a}^{t_b} (\mathbf{E} + \mathbf{v} \times \mathbf{B})\, dt \tag{1.5}$$

where $\mathbf{E}$ and $\mathbf{B}$ are the electric and magnetic fields generated by the kicker along the path. On that same path the particle will undergo an energy change

$$\Delta E = e\int_a^b \mathbf{E} \cdot d\mathbf{s} \tag{1.6}$$

To calculated the *transverse* kick using Eq. 1.5 requires knowledge of both the (transverse) electric and magnetic fields. However, the Panofsky-Wenzel theorem shows that for time-varying electromagnetic fields, the deflection can be expressed in terms of only the *longitudinal* component of the kicker's electric field; the original derivation of the theorem [14] was for fields with sinusoidal time dependence, but was later extended [10] to any time-varying field. In many instances this theorem can be used to simplify not only the calculation of transverse effects, but of one's conceptualization of them, as well.

We now make the assumption, which we will employ throughout virtually all the succeeding sections, that the particles move with *constant velocity* (see Appendix 1), i.e., that the trajectory from a to b is a straight line in the z-, or equivalently, the s- direction, which is traversed at constant speed $v = \beta c$. This implies that the time and (longitudinal) position coordinates along the path are related by

$$s = a + v(t - t_a) \tag{1.7}$$

For a full discussion of the coordinates and integration limits in equations such as Eqs. 1.5 and 1.6, the reader is referred to Appendix 2.

If we now differentiate Eq. 1.5 with respect to time (the differentiation is actually with respect to t_a; see Appendix 2), under the constant velocity approximation, we obtain

$$\frac{\partial \Delta\mathbf{p}}{\partial t} = e\left[\int_{t_a}^{t_b} \frac{\partial \mathbf{E}}{\partial t}\, dt + \int_a^b d\mathbf{s} \times \frac{\partial \mathbf{B}}{\partial t}\right] \tag{1.8}$$

If we insert

$$\frac{\partial \mathbf{B}}{\partial t} = -\nabla \times \mathbf{E} \tag{1.9}$$

and use the identity

$$d\mathbf{s} \times \nabla \times \mathbf{E} = \nabla (d\mathbf{s} \cdot \mathbf{E}) - (d\mathbf{s} \cdot \nabla)\mathbf{E}$$

$$= \nabla (d\,\mathbf{s} \cdot \mathbf{E}) - \frac{\partial \mathbf{E}}{\partial s} ds \tag{1.10}$$

we can combine the space and time partial derivatives of **E** to obtain

$$\frac{\partial \mathbf{p}}{\partial t} = e \int_a^b \left[-\nabla (d\,\mathbf{s} \cdot \mathbf{E}) + d\,\mathbf{E} \right] \quad . \tag{1.11}$$

Eq. 1.11 can be separated into longitudinal and transverse components to yield

$$\frac{\partial}{\partial t} (\Delta p_s) = e \frac{\partial}{\partial t} \int_{t_a}^{t_b} \mathrm{E}_s \, dt \tag{1.12a}$$

and

$$\frac{\partial}{\partial t} (\Delta \mathbf{p}_\perp) = - e \int_a^b \left[\nabla_\perp (\mathbf{E} \cdot d\,\mathbf{s}) - d\mathbf{E}_\perp \right] \quad , \tag{1.12b}$$

where the operator $\nabla_\perp$ denotes the transverse components of the gradient. The latter equation is the one of interest. Evaluating the integral, and making use of Eq. 1.6 yields

$$\frac{\partial}{\partial t} \Delta \mathbf{p}_\perp = - \nabla_\perp (\Delta E) + e \ [\mathbf{E}_\perp(b,t_b) - \mathbf{E}_\perp(a,t_a)] \tag{1.13}$$

which is the result for arbitrary time dependence. As we saw in the discussion of the reciprocity theorem, we can usually choose a and b to represent points at which the entrance and exit fields vanish, and so the term in the square brackets is zero. Finally, if we consider fields with sinusoidal variation $e^{j\omega t}$, and divide by the electron charge e, we get the original form of the Panofsky-Wenzel theorem,

$$\boxed{\frac{j\omega \Delta \mathbf{p}_\perp}{e} = -\frac{1}{e} \nabla_\perp (\Delta E) = - \nabla_\perp V}, \tag{1.14}$$

where we define $V \equiv \Delta E/e$ as the beam voltage gain, in this case resulting from the energy change produced by the longitudinal field of the kicker.

There are several points worth noting about Eq. 1.14. First, as advertised, we have obtained an expression for the *transverse* kick purely in terms of the *longitudinal* electric field (except perhaps for an additional static deflection). Surprisingly, this implies that it is *not* possible to produce a transverse deflection in a kicker which has *only* a transverse component of electric field (i.e. if the kicker is excited in a TE or TEM mode)! This apparently paradoxical conclusion results from the fact that in such a mode, the deflection due to the $\mathbf{v} \times \mathbf{B}$ force will exactly cancel that due to the transverse **E** field.

A corollary of the above result is that a transverse kicker generates a transversely varying longitudinal kick which introduces an energy gradient across the width of the beam.

However, since it is only the transverse *gradient* of the longitudinal field which causes the deflection, it is usually possible to find a mode of excitation for a deflecting kicker in which the field on the longitudinal axis is zero, so that after multiple passes (e.g. in a cyclic accelerator), the energy gain for all particles averages to zero.

As implied by the above remarks, the Panofsky-Wenzel theorem is a statement about an electrode system *in a particular mode of excitation.* In fact the same electrode system can function as either a longitudinal or a transverse kicker, depending on the mode of excitation. (We note parenthetically that this is not always desirable: An rf cavity, a longitudinal kicker when excited at its fundamental frequency, may also experience excitation of higher-order modes, some of which may provide unwanted transverse deflections.) Putting the matter somewhat more concisely: The Panofsky-Wenzel theorem does *not* predict the behavior of a electrode system when it is excited as a transverse kicker based on its behavior when it is excited as a longitudinal kicker; rather, for a given mode of excitation, it enables us to calculate its transverse effect on the beam based on its longitudinal effect on it.

Finally, we note the significance of the terms j and ω in Eq. 1.14. The presence of the latter shows that for a given magnitude of transverse gradient, the higher the frequency at which the kicker is excited, the less of a transverse kick it imparts. The presence of the former term indicates that the transverse kick occurs 90° out of phase with the longitudinal one. For a transverse kicker in the form of a standing-wave cavity this is relatively easy to see: In the TM excitation of such a cavity, the transverse magnetic field, which is usually the principal agent of the transverse kick, is 90° out of phase with the longitudinal electric field.

2. The Beam Voltage

Thus far, our definition of $1/e$ times the energy gain as a beam "voltage" has been a notational convenience. The fact that the transverse gradient of that quantity is proportional to the transverse kick suggests that there may actually be a physical basis to regarding it as a voltage. (In fact, one of the principal motivations for calculating the beam voltage *is* to enable us to calculate the transverse kick.) We shall now show that the beam voltage can be regarded as a two-dimensional scalar field (it has no z-dependence, as may be seen from Eq. A.2.10 in Appendix 2) and is in fact the solution of a two-dimensional equation which, for highly relativistic particles, reduces to Laplace's equation. Hence, the problem of calculating the spatial variation of an electrode's effect across its aperture can reduced from an integration over a three-dimensional distribution of field waves, to the solution of a two-dimensional boundary-value problem.

As we have seen, under the constant-velocity approximation the energy increment given to a particle passing through a kicker depends only on the transverse coordinates and the time, i.e., if expressed as a voltage V it has the form

$$V(x,y,t) = \int_a^b \mathbf{E} \cdot d\mathbf{s} \quad . \tag{2.1}$$

In the integration, the value of $\mathbf{E} = E_z$ must be taken at the time $t = t_a + (s - a)/\beta c$, so that the time on which V depends is actually the time that the particle arrives at the kicker, t_a. For simplicity, let us omit the subscript z, and then note that this z- (or s-) component must satisfy the wave equation

$$\nabla^2 E - \frac{1}{c^2}\frac{\partial^2 E}{\partial t^2} = 0 \ . \tag{2.2}$$

Let us now use the above to find a two-dimensional differential equation for V involving the quantity

$$\nabla_\perp^2 V \equiv \frac{\partial^2 V}{\partial x^2} + \frac{\partial^2 V}{\partial y^2} \ . \tag{2.3}$$

If we differentiate Eq. 2.1 and insert Eq. 2.2 we obtain

$$\nabla_\perp^2 V \equiv \int_a^b \left(\nabla_\perp^2 E\right) ds = \int_a^b \left(\frac{1}{c^2}\frac{\partial^2 E}{\partial t^2} - \frac{\partial^2 E}{\partial s^2}\right) ds \tag{2.4}$$

As noted in Appendix 2, any partial derivatives appearing under the integral sign are taken *prior to* making the substitution for t in terms of s. After the substitution, E will be a function of the form $f[s,t(s)]$. Taking the expression for the total differential of such a function in terms of its partial derivatives, integrating, and rearranging terms gives

$$\int \frac{\partial f}{\partial s} ds = f - \int \frac{\partial f}{\partial t}\frac{dt}{ds} ds + const \ , \tag{2.5}$$

Applying this result to the integration of the second term of Eq. (2.4) we obtain

$$\nabla_\perp^2 V = -\left.\frac{\partial E}{\partial s}\right|_a^b + \int_a^b \left(\frac{1}{c^2}\frac{\partial^2 E}{\partial t^2} + \frac{1}{\beta c}\frac{\partial^2 E}{\partial s\,\partial t}\right) ds \tag{2.6}$$

If we again apply Eq. 2.5 to integrate the mixed-derivative term we obtain

$$\nabla_\perp^2 V = \left(-\frac{\partial E}{\partial s} + \frac{1}{\beta c}\frac{\partial E}{\partial t}\right)\Bigg|_a^b - \frac{1}{(\beta\gamma c)^2}\int_a^b \frac{\partial^2 E}{\partial t^2} ds \ . \tag{2.7}$$

Substituting using Eq . 2.1 and rearranging terms we get

$$\nabla_\perp^2 V + \frac{1}{(\beta\gamma c)^2}\frac{\partial^2 V}{\partial t^2} = \left(-\frac{\partial E}{\partial s} + \frac{1}{\beta c}\frac{\partial E}{\partial t}\right)\Bigg|_{a,\ t_a}^{b,\ t_a + (b-a)/\beta c} \tag{2.8}$$

The notation for the limits is to serve as a reminder that after taking the partial derivatives, one must substitute the appropriate $t(s)$.

The solution of Eq. 2.8 is the desired function. As was the case with the previous theorems, it is usually possible to choose the limits a and b to be locations where the fields are zero (or alike), making the right hand side zero; Eq. 2.8 then simplifies to a

modified form of the wave equation

$$\nabla_{\perp}^2 V + \frac{1}{(\beta\gamma c)^2}\frac{\partial^2 V}{\partial t^2} = 0 \quad . \tag{2.9a}$$

For the case of fields with a sinusoidal $e^{j\omega t}$ dependence, Eq. 2.9a is further simplified

$$\nabla_{\perp}^2 V - \left(\frac{k}{\gamma}\right)^2 V = 0 \tag{2.9b}$$

where $k = \omega/\beta c$ is the *beam* wave number.

Recall that the fields which result in the energy gain are produced by the kicker fields, and are independent of the beam. The only manifestation of the beam is in the presence of the $\beta\gamma$ term, which arises from the relation of s and t along the path, in particular, from the degree to which it differs from c. In fact, for highly relativistic particles, Eq. 2.9b approaches Laplace's equation, and determining V reduces to solving an electrostatics problem.

The solution to an equation such as 2.9b is determined by the values at the boundary. To understand what this means in practical terms, we shall see in the following sections of this report that for many electrode systems, the electrodes are located very near the walls of the beam enclosure. In the case of the prototypical parallel-plate electrodes, such electrodes might actually form a part of the wall, albeit electrically isolated from it by thin accelerating gaps. (Such a wall would perforce be part of a rectangular enclosure; a more common configuration would involve a cylindrical enclosure such as a beam tube, with the electrodes constituting portions of the cylinder.)

Let us consider the somewhat artificial situation of long plates and focus our attention on either the entrance or exit gap alone. If the end gaps are sufficiently narrow that they have a transit-time factor of ≈ 1 (see Appendix 2), then a particle passing very near the electrode surface (i.e., at the beam-aperture boundary) will experience at the entrance (exit) gap, a beam voltage change equal to the negative (the value) of the instantaneous voltage across that gap. In other words, for an electrode essentially flush with the beam tube wall, the boundary value of the beam voltage is, apart from a possible transit-time factor, just the voltage on the electrode, and so the cross-sectional profile of the beam voltage (for a highly relativistic particle) is just what we would get by solving a simple two-dimensional electrostatics problem with that portion of the wall subtended by the electrode set at the electrode voltage!

Applying the above results in conjunction with Green's reciprocation theorem leads to the following strikingly simple result: The g-factor, which we originally defined as the fraction of the beam charge appearing on the electrode, was calculated by finding the potential at the beam position with the electrode at unit potential. Since that voltage turns out to be the boundary value for the beam voltage problem, we see that the g-factor also represents the fraction of the beam voltage at the wall that is experienced by a particle at the actual beam position (one more striking demonstration of the reciprocal relation between pickups and kickers).

3. Frequency Spectrum of a Charged-Particle Beam

Having made frequent reference to the frequency domain, and the fact that the beam currents that enter into many equations are sinusoids, it behooves us to talk about the decomposition of particle-beam currents into such sinusoids, i.e. to talk about the frequency spectra of such beams. Excellent and detailed discussions of beam spectra can be found in Refs [1] and [15]. We will therefore merely summarize the important results here and accompany them with some quasi-hand-waving in the hope of giving the reader some physical feeling for them.

a, Single-Particle Spectrum

i. Longitudinal Spectrum. The spectrum of a beam is simply the superposition of the signals of the individual particles. If we consider a single particle circulating in a circular accelerator at frequency f_{rev}, a longitudinal pickup at a fixed location will simply see a current that is a periodic delta function in time, which can expanded as a Fourier series (i.e. expressed in the frequency domain) to yield

$$i(t) = \sum_{m=-\infty}^{\infty} \delta(t - mT_{rev}) = e f_{rev} \sum_{n=-\infty}^{\infty} e^{jn\omega_{rev}t} = e f_{rev} + 2e f_{rev} \sum_{n=1}^{\infty} \cos(n\omega_{rev}t) \quad (3.1)$$

The frequency spectrum of such a "beam" will show, along with the expected d.c. current ef_{rev}, a current of peak amplitude $2ef_{rev}$ at *every integer multiple* of f_{rev}.

Eq. 3.1 describes the frequency spectrum characterizing a particle of fixed revolution frequency, or fixed energy, such would occur for a "coasting" beam, i.e. for motion in the absence of any r-f bunching (including that due to a stationary r-f bucket). In the presence of r-f, the revolution frequency of a particle with energy differing by ΔE from the orbit reference energy E, will vary over a range of $\Delta f = \pm \eta f_{rev} \Delta E/E$ due to its synchrotron motion. (Because this variation occurs at the particle's synchrotron frequency ν_s, the revolution frequency is *frequency-modulated* at ν_s; hence, the single-particle spectral lines are not smeared out continuously over the range Δf, but are rather split into a series of so-called satellite lines which span the range Δf, and are separated by ν_s, characteristic of f-m spectra.)

ii. Transverse spectrum. A *transverse* pickup (with a linear response to transverse displacement) will sense the particle's dipole moment, which can have both a time-independent part (due to a "dc" offset of the orbit relative to the center of the pickup) as well as a time-varying part (due to the particle's betatron motion). The latter is generally of more interest, and we consider it first.

If the particle's betatron motion is characterized by an amplitude A and tune Q (i.e. betatron frequency Qf_0), the pickup will see a time-dependent dipole moment given by

$$\begin{aligned} d(t) &= e f_{rev} \sum_{n=-\infty}^{\infty} e^{jn\omega_{rev}t} \times A \cos Q\omega_{rev}t \\ &= Ae f_{rev} \left[\sum_{n=0}^{\infty} \cos n\omega_{rev}t(n+q) + \sum_{n=1}^{\infty} \cos n\omega_{rev}t(n-q) \right] \end{aligned} \quad (3.2)$$

where q is the fractional part of Q. Note that in contrast to Eq. 3.1, where the signals at positive and negative frequencies combined to produce a signal of twice the amplitude at the positive (i.e. detectable) frequency, due to the presence of the q term, the negative- frequency terms occur at different frequencies from the positive ones. Hence, the betatron motion produces two lines per frequency interval f_{rev} in the transverse spectrum. Using communication theory language, the transverse pickup observes a signal whose amplitude is modulated at the betatron frequency (see the first line of Eq. 3.2), producing a pair of a–m sidebands. In addition, if the particle's equilibrium orbit is displaced by an amount A_O from the detector center, there will be additional lines of amplitude $2A_O e f_{rev}$ at each integer multiple of f_{rev}. It is standard parlance to refer to the former signals as betatron lines, and the latter, as revolution or common-mode lines. As with the case of the longitudinal signals, the transverse-detector signals will exhibit splitting into synchrotron satellites.

b. Bunched-Beam Spectrum

If we now consider a beam consisting of a single bunch of N such particles, we may, to first order, treat it as a giant superparticle of charge Ne, i.e., having the same spectrum, but with each spectral component having N times the amplitude. In actual fact, the situation is somewhat more complex. Unlike the idealized delta-function density, the bunch will have a finite time width τ, and so the frequency spectrum, rather than exhibiting the above infinite extent, will begin to roll off at frequencies on the order of $f \sim 1/\tau$. In the Fermilab Tevatron, where the bunch width is on the order of 1-2 nsec, this so-called single-bunch roll-off frequency is several hundred MHz; in a machine such as the new LBL Advanced Light Source, with pulses on the order of 30 psec, the roll-off frequency is about 10 GHz.

As with the single-particle, the bunch will exhibit longitudinal and transverse oscillations. However, the amplitudes of the oscillations will be those associated with the beam as a whole, the superparticle, and so will be much smaller than those of most of the individual particles; hence the spectral linewidths of these coherent signals will be smaller than those associated with the individual particle signals. This should become clearer following the discussion in the next section.

If we neglect for the moment the frequency distribution *within* the individual lines (equivalent to assuming a detector with a frequency resolution greater than the linewidth) it follows from Eq. 3.1 that, below the bunch roll-off frequency, at each harmonic of the revolution frequency, a single N-particle bunch generates at each revolution harmonic an effective current of peak amplitude

$$I_o(\omega) = 2Nef_{rev} = 2\,I_{dc} \tag{3.3}$$

The mean-square current, relevant for questions of signal power, will be given by

$$\langle I^2(\omega)\rangle = \frac{1}{2} I_o^2(\omega) = 2N^2 e^2 f_{rev}^2 \tag{3.4}$$

Were the same N particles to be divided equally into n equally spaced identical bunches, to a fixed pickup the situation would be identical to having a single bunch of N/n particles circulating at frequency nef_{rev}, giving a frequency spectrum with $1/n$ times the number of lines (i.e., only at frequencies which are multiples of nf_{rev}), but with the same peak current per line. Hence the average signal power would be down by $1/n$–as

one can readily see in the time-domain picture. For unequal bunch populations or bunch spacings, signals of varying amplitude would again appear at the intermediate multiples of f_{rev}, the amplitude distribution depending on the details of the bunch pattern.

Analogously, for a single N-particle bunch with a *coherent* betatron amplitude A, the "dipole current" is given by

$$d_o(\omega) = I_o(\omega)\, A = ANef_{rev} \tag{3.5}$$

and the equivalent mean-square quantity is

$$\langle I^2(\omega)A^2\rangle = \frac{1}{2} I_o^2(\omega)\,\frac{A^2}{2} = \frac{1}{4} A^2 N^2 e^2 f_{rev}^2 \tag{3.6}$$

c. Schottky Spectrum

In an unbunched, or coasting beam, we find that, as in the case of a bunched beam, for a beam of N particles one observes a d-c current which is N times the single-particle current. What is perhaps surprising is that there are also a-c signals (known as Schottky signals, after the man who first predicted their existence) produced by the *fluctuations* in this current, and that these signals occur at the same frequencies as the single particle signals.

A somewhat oversimplified explanation of this is as follows. In a bunched beam, the signals from the N individual particles add coherently (i.e., in phase) to produce a current which is N times the single-particle current, and hence will produce a signal power which is N^2 times that of a single particle. In a coasting beam, the signals from the individual particles are uncorrelated and so the phases of their relative signals (except for their d-c signals, which have no phase) are uncorrelated. Hence when the signals are combined, they "add" in an rms sense rather than linearly, and so the total signal power will be only N times that of a single particle. For this reason one generally refers only to mean-square quantities when discussing Schottky signals. For such signals, the longitudinal mean-square current is given by

$$\langle I_S^2(\omega)\rangle = 2Ne^2 f_{rev}^2 \tag{3.7}$$

We have introduced the quantity $\langle I_S^2(\omega)\rangle$ to permit us in subsequent sections to write formulas for signal power which can be applied to both coherent and Schottky signals. Similarly we can write the Schottky counterpart to Eq. 3.6

$$\langle d_S^2(\omega)\rangle = \langle I_S^2(\omega)x^2\rangle = Ne^2\langle f_{rev}^2\, x^2\rangle \tag{3.8}$$

Note that the Schottky dipole current depends on the mean-square beam dimensions.

The utility of Schottky signals results from the fact that they reflect the behavior of the individual particles rather than the beam as a collective entity, and that they are present even when the beam is in an "unperturbed" state. In the case of Eq. 3.8, the strength of the Schottky signal seen in a transverse detector reflects the excursions of the individual particles, which are present even in a perfectly centered beam, rather than the oscillation of the beam centroid. Similarly, the frequency spread of the longitudinal signals represents the energy excursions of the individual particles, rather than the energy excursions of the beam centroid, a consequence of imperfect centering in the rf bucket.

The principal problem in detecting Schottky signals is their relative weakness. In most accelerators, the beam is bunched, and a comparison of the equations for mean-square signals (upon which we will see that detector signal power depends) in the above two sections shows that with N particles in the machine, the coherent signal produces on the order of N times the power of the Schottky signal. For a typical accelerator, N will be on the order of 10^{10} or greater, and so most attempts to observe Schottky signals from bunched beams have, despite great effort, been unsuccessful. We present below the results one of the few successful attempts [16], primarily because it illustrates many of the concepts we have been discussing.

Observation of a Schottky signal in a bunched beam machine requires suppression of the coherent signal by many orders of magnitude. In the experiment we describe, performed at the Fermilab Tevatron, use was made of the fact that the coherent signal starts to decrease above the single-bunch roll-off frequency, the rate of fall-off depending on the details of the beam bunch shape. Because of the small size of the Schottky signals the pickup employed needed to be a high-gain device, for which purpose a high-Q resonant cavity[2] was employed. As noted earlier, the roll-off frequency for the Tevatron is several hundred MHz, whereas the beam-tube cutoff frequency (the highest frequency at which the cavity can function as a high-Q resonator) is about 2.5 GHz. The resonant frequency of the cavity was therefore designed to be roughly 2 GHz.

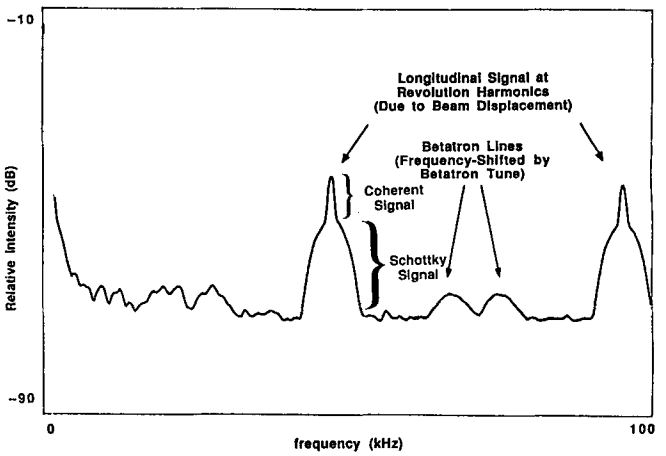

Fig. 4 Actual Schottky spectrum obtained at the Fermilab Tevatron

The observed spectrum is shown in Fig. 4. Two features should be pointed out immediately: The intensity scale is logarithmic, and the frequency scale has an offset of over 2 GHz. The cavity is excited in a mode which responds to the beam's dipole moment, and so, because the beam is not perfectly centered within the cavity, one sees revolution lines as well as betatron lines. The former, the large peaks at roughly 50 and 100 kHz, are actually spaced by 47.11 kHz, the Tevatron revolution frequency.[3]

Note that the revolution lines are actually compound peaks–a narrow, intense peak atop a broad, weaker one. The former are due to the residual coherent signal; the latter, the

[2]We will discuss in some detail the nature of such a device in Section 7 of this report.

[3]The two peaks actually correspond to revolution harmonic numbers 42,892 and 42,893.

longitudinal Schottky signal. The relative intensities of the peaks indicate a that at 2 GHz, the coherent signal has fallen by over 80 dB. Had the beam had a Gaussian longitudinal profile, this suppression would have been hundreds of dB; the observed suppression is more like what one would expect from a profile resembling a "cosine-squared" distribution. As noted earlier, the greater breadth of the Schottky line reflects the momentum excursion of the individual particles within the beam, whereas the lesser width of the coherent signal reflects only the momentum excursion of the beam centroid.

The two peaks appearing between the two revolution lines are the betatron signals. Their line widths are comparable to those of the broad peaks in the revolution lines, but there is no evidence of the narrow peak, indicating that they are pure Schottky signals, uncontaminated by any coherent signal. The reason for the additional coherent-signal suppression in the betatron lines is that, as seen from Eqs. 3.6 and 3.8, the ratio of coherent to Schottky mean-square dipole moment also depends on the ratio of the mean-square coherent betatron amplitude to the mean-square beam size; under the conditions that the spectrum was recorded, the former that ratio was something less than 50 dB.

d. Summary of Qualitative Results.

We see that the longitudinal frequency spectrum of a beam is characterized by signals occurring in discrete frequency bands centered about frequencies which are integer multiples of the revolution frequency f_{rev}; if the beam is bunched by an r-f system operating at nf_{rev} and there is a nearly uniform population of the r-f buckets, strong signals will be present in or near those bands which are integer multiples of nf_{rev}, with weaker signals at the other revolution harmonics. These signals will begin to roll off at frequencies characteristic of the bunch length. A second set of longitudinal signals, the Schottky signals, caused by particle-to-particle fluctuations in beam intensity and producing a signal power reduced in power by a factor of N, is present in both bunched and unbunched beams.

A transverse detector will also see signals at the above frequencies for a beam which is offset relative to the detector. In addition, it will see signals at pairs of frequencies intermediate to the revolution harmonics, due to the betatron motion of the particles. For bunched beams, a coherent betatron signal will be observed only if the beam is experiencing a coherent betatron oscillation; in contrast, Schottky betatron signals are present for any beam of finite width. Like the coherent longitudinal signals, coherent betatron signals roll off at frequencies characteristic of the bunch length.

As a final point we note that although the coherent signals due to the individual bunches roll off at the above frequency, signals characteristic of motion *within* the bunch (such as would be produced by single-bunch instabilities) will appear at frequencies which are perforce at higher frequencies than this. The presence of such frequencies in the observed spectrum will therefore be indicative of such intra-bunch oscillations.

4. Figures of Merit for Kickers and Pickups

The parameters which we will use to describe the coupling between the input/output terminals of a pickup/kicker and the beam are all defined in the frequency domain. Hence in the following section, all currents and voltages are to be understood as complex phasor quantities, as described above. We begin by discussing the response functions for kickers, using the Panofsky-Wenzel theorem to relate the longitudinal and transverse behavior. We then define the response functions for pickups, and finally, relate the two sets of responses using the Lorentz reciprocity theorem.

a. Kicker Response Functions

i. The Kicker Constant. Perhaps the most "natural" figure of merit for a longitudinal kicker is the quantity known as the kicker constant, which is simply the dimensionless ratio of change in the beam voltage to the input voltage V_K

$$K_{\|} \equiv \frac{\Delta E/e}{V_K} = \frac{V}{V_K} \tag{4.1}$$

The expression for V is given by Eq. 2.1; as shown in Eq. A.2.10 (Appendix 2), under the constant velocity approximation and assuming the accelerating field to be a phasor, V can be written, apart from a phase factor, as

$$V = \int_a^b E_s \, e^{jk_B s} \, ds \tag{4.2}$$

To reiterate statements made elsewhere: The exponential factor in the integrand results from expressing t in the time-dependent phasor as a function of the position along the path; both E and V will generally depend on the transverse coordinates (E will also generally depend on the longitudinal coordinate; V cannot).

For a longitudinal accelerating device such as an r.f. cavity, it is common to compare the change in beam voltage with the instantaneous cavity voltage V_O, defined (again, apart from a phase factor) as

$$V_o = \int_a^b E_s \, ds \tag{4.3}$$

The ratio of the change in beam voltage to V_O is known as the transit-time factor T, which is then seen to be given by

$$T = |V/V_o| = K_{\|} \, V_K/V_o \tag{4.4}$$

As the name implies, T simply represents the reduction in energy gain due to the fact that, because of the finite transit time of the beam through the kicker, it may not experience the (time-) maximum field everywhere along its path (see Appendix 2 for a somewhat lengthier discussion of this factor).

To define a transverse kicker constant, we need a transverse equivalent to the beam voltage. As pointed out in Appendix 1, under the constant velocity approximation

$$\Delta E = \beta c \, \Delta p_{\|} \tag{4.5}$$

It is therefore reasonable to adopt as the *transverse* beam voltage $\beta c \, \Delta p_{\perp}/e$, whereupon we can define the transverse kicker constant as

$$K_{\perp} \equiv \frac{\Delta p_{\perp} \beta c}{e V_K} \tag{4.6}$$

where is is understood that $K_\perp$ (and equivalently $\Delta p_\perp$)can indicate either of the transverse directions. One can calculate $K_\perp$ directly by substituting into Eq. 4.6 the perpendicular components of $\Delta \mathbf{p}$ as given by Eq.1.5. A simpler approach is to calculate the (longitudinal) beam voltage *for the mode in which the device is excited as a transverse kicker* and use the Panofsky-Wenzel theorem, Eq. 1.14, to calculate $\Delta p_\perp$. Combining Eqs.1.14 , 4.1, and 4.6 gives us

$$K_\perp = -\frac{1}{jk_B} \nabla_\perp K'_\parallel \quad . \tag{4.7}$$

We use the prime symbol ('), here and elsewhere, to indicate transverse excitation, particularly in those cases where the perpendicularity symbol might either complicate or confuse the notation. Its presence in $K'_\parallel$ is to serve as an explicit reminder that the transverse kicker constant is *not* obtained from the transverse derivative the "usual" longitudinal kicker constant (i.e., the kicker constant associated with the excitation of the device as a longitudinal kicker). In terms of our paradigm of the parallel-plate electrodes, the kicker constant we refer to as $K_\parallel$ would be calculated from the (longitudinal electric) fields which result when the plates are excited with equal voltages (of the same sign); $K'_\parallel$, from the fields when they are excited with equal voltages of opposite sign.

ii. Shunt Impedance The drawback in K as a figure of merit is that it reflects the impedance of the input circuit as well as the intrinsic behavior of the kicker electrodes: One can make the kicker *appear* to be, say, twice as efficient (in terms of its K) by quartering its input line impedance, and building in an internal transformer to attain the same ΔE (or Δp) with half as much input voltage; however the true efficiency of the kicker, which is reflected in the ratio of ΔE to the voltage *on the kicker electrodes* (which depends on the nature of the electrodes themselves, and not on the impedance of the input cable) would be unchanged.

In seeking a better, if somewhat less intuitive, figure of merit than K, let us borrow from the practice used for r-f cavities in which a shunt impedance is *defined* to relate cavity voltage (Eq. 4.3) and power according to

$$R \equiv |V_o|^2 / 2P \tag{4.8}$$

For the kicker, we are most interested in the *beam* voltage, $V = V_o T$, which suggests the relation

$$P = |V_o\, T|^2 / 2RT^2 = |V|^2 / 2RT^2 \tag{4.9}$$

in which we call the quantity RT^2 the kicker shunt impedance. For convenience, this quantity is sometimes shortened to RT^2, or simply R; however, we shall use the expression $R_\parallel T^2$ to make it clear that it contains the transit-time factor and refers to the longitudinal action of the kicker we will shortly define a similar quantity related to transverse motion).

It is this quantity $R_\parallel T^2$ which proves to be the operative figure of merit for a kicker. The reason is that it relates the change in beam voltage to the input power, a quantity which is independent of any input transformer, and hence is a measure of the "efficiency" of the kicker. Moreover, looking back to the individual definitions of $R_\parallel$ and T, we see that both of these quantities relate to the field within the actual kicker electrodes, and not the details

of the input circuit; we will see this feature more explicitly when we calculate values of $R_{\|}T^2$ for particular devices in some of the following sections.

To relate the shunt impedance to the kicker constant, we note that the input power is given by $V_k^2/2Z_c$, where Z_c is the characteristic impedance of the input line. Substituting for V_o using Eq. 4.4, we obtain the result

$$R_{\|}T^2 = Z_c |K_{\|}|^2 \tag{4.10}$$

We can, in like fashion, define a transverse shunt impedance. In this case we relate the input power to the *transverse* beam voltage, which we have defined as $\beta c\, \Delta p_{\perp}/e$. Following an approach similar to that used above, we arrive at the result

$$R_{\perp}T^2 \equiv \left| \Delta p_{\perp} \beta c /e \right|^2 /2P = Z_c |K_{\perp}|^2 \tag{4.11}$$

In this definition, the transverse shunt impedance has the dimensions of a resistance, as is needed for kicker power calculations. This convention is used is the URMEL codes for calculating cavity responses. However, an alternative, and often used, definition uses the product $R_{\perp}T^2 \cdot k_o$, which has the dimensions of resistance/length (i.e., displacement).

b. Pickup Response Functions

i. The Transfer Impedance. Referring back to the Introduction, in particular to Fig. 2a, we can see that for a longitudinal pickup, the "natural" figure of merit would be the ratio of the pickup output voltage to the beam current. By definition, such a quantity would have the dimensions of an impedance which, for obvious reasons, is called the longitudinal *transfer* impedance, and the defining relation is simply

$$Z_P \equiv V_p/I_B \tag{4.12}$$

For a transverse pickup, the corresponding quantity would be the ratio of the output voltage to the beam's dipole moment; by analogy it is also called a transfer impedance, although its dimensions are actually impedance divided by length. The relation for the transverse transfer impedance is then

$$Z_P' \equiv V_P'/I_B\, \Delta x \tag{4.13}$$

where, by definition, V_P' is a voltage proportional to the dipole moment of the beam; as we did previously, we use the prime (') symbol to denote transverse characteristics.

ii. Relation Between Pickup and Kicker Characteristics. Like the kicker constant, the transfer impedance suffers from the fact that it depends on the output circuit impedance as well as on the intrinsic efficiency of the pickup. One could employ the same remedy as in the kicker case by defining a pickup shunt impedance. However, since any device which acts as a pickup can also act as a kicker, rather than defining yet another impedance, a more useful approach is to make use of the relations between pickup and kicker behavior, which we obtained using the Lorentz reciprocity theorem, to characterize a pickup in terms of the corresponding *kicker* shunt impedance.

As a first step, we use that result to relate the longitudinal and transverse transfer impedances to the respective kicker constants. If we insert Eq. 1.2 in Eq. 4.12, we obtain

for the longitudinal transfer impedance

$$Z_p = -\frac{Z_c}{2V_K I_B} \int_{\text{vol (at fixed time)}} \mathbf{E_K} \cdot \mathbf{J_B}\, d\, vol \tag{4.14}$$

In this volume integral, values of $\mathbf{E_K}$ and $\mathbf{J_B}$ are taken at a fixed time. The beam, assumed to be moving in the positive s-direction with velocity βc, will have an s-dependence e^{-jks}. (As noted in Appendix 2, this term does not arise from substituting the appropriate value of s into the exponential time dependence, but rather represents the spatial dependence of a sinusoidal wave propagating in the $+s$ direction.) Furthermore, assuming $\mathbf{E_K}$ does not vary greatly over the beam cross section, we may integrate over x and y giving

$$\int_{\text{beam area}} \mathbf{E_K} \cdot \mathbf{J_B}\, dxdy = \mathbf{E}_K \cdot \mathbf{I_B}\, e^{-jks} \quad . \tag{4.15}$$

whence Z_p becomes

$$Z_p = -\frac{Z_c}{2V_K} \int_{\text{beam path}} e^{-jks}\, \mathbf{E_K} \cdot d\, \mathbf{s} \tag{4.16}$$

This integral differs from that in Eq. 4.2 defining $K_{\|}$ only in the sense of s. Therefore, it represents a kicker excited with V_K, but with the beam waves traveling in the sense opposite to that when the device is employed as a pickup. This is not merely mathematical sleight of hand: For electrode systems which exhibit directional behavior (e.g., striplines) the direction in which the beam passes when the device operates as a pickup must be opposite that which it does when the device acts as a kicker. The relation between pickup and kicker responses for a given electrode is therefore

$$Z_p = \frac{1}{2} Z_c\, K_{\|} \tag{4.17}$$

with the provision that the beam sense be reversed between the two applications.

The corresponding relation for transverse responses is obtained by differentiating Eq. 4.17 with respect to x,

$$Z_p' = \frac{1}{2} Z_c \frac{\partial K'_{\|}}{\partial x} \tag{4.18}$$

where we again use the prime to note that the kicker is excited in the transversely deflecting mode. We can then use Eq. 4.7 to obtain

$$Z_p' = -\frac{1}{2} jk_B Z_c K_{\perp} \tag{4.19}$$

Having obtained the relation between the transfer impedances and the respective kicker constants, we are now in a position to use Eqs. 4.10 and 4.11 to characterize the pickup output in terms of the kicker shunt impedance. The power from the pickup signal into an impedance-matched load, Z_C is

$$P_p = \langle I_B^2 \rangle Z_p^2 / Z_c \tag{4.20}$$

(We have used the notation $\langle I_B^2 \rangle$ for the mean-square current, rather than the explicit $I_B^2/2$ for sinusoidal currents, so that the expressions here may be easily applied to the case of Schottky signals; see Sect. 3.) We may rewrite Eq. 4.19 in terms of the electrode's (kicker) shunt impedance using Eqs. 4.17) and 4,9 to obtain, for the longitudinal pickup,

$$P_p = \langle I_B^2 \rangle R_{\parallel} T^2/4 \tag{4.21}$$

Here we see that the shunt impedance (modified by the factor 1/4) serves equally well as a measure of efficiency of that electrode used as a pickup. Similarly, for the transverse pickup, we obtain the power

$$P_p' = \langle I_B^2 x^2 \rangle k_B^2 R_{\perp} T^2/4 \tag{4.22}$$

The appearance of the beam wave number $k_B = \omega/\beta c = 1/\beta\lambda\!\!\!^{-}$ in the transverse response means that, when acting as a kicker, a given electrode configuration will exhibit an efficacy which is reduced at higher frequencies relative to its performance as a pickup. With this qualification, we see that high shunt impedance relates to high efficiency for an electrode whether used as a pickup or a kicker.

Finally, having established the shunt impedance as a figure of merit for pickups as well as kickers, it makes sense to write down the relations between transfer and shunt impedance. Combining Eqs. 4.10 and 4.11 with Eqs. 4.17 and 4.19, respectively gives

$$Z_p = \sqrt{Z_c R_{\parallel} T^2}/2 \tag{4.23}$$

and

$$Z_p' = k_B \sqrt{Z_c R_{\perp} T^2}/2 \tag{4.24}$$

A summary of the useful relations for beam electrodes is presented below in Table I.

c. Effect of Impedance Mismatch

In applying the reciprocity-derived relations, we have assumed that the voltages V_k and V_p were observed at an impedance-matched connection where no reflected waves were present. This is not always the case in practice, and mismatch introduces some modification in the relations we have derived.

Impedance mismatch most often occurs for a resonant electrode such as a cavity. Without connection to a driver or amplifier input impedance, such an electrode is characterized by an unloaded Q-value, Q_U. With driver or load attached, the total circuit response is widened to $\Delta\omega/\omega = Q_L$ which depends on the load and how it is coupled to the electrode. (In some applications the degree of loading may conveniently be used to adjust the response width.) At the terminals of a kicker, of course, the driver impedance has no effect on K or RT^2, but the overall efficiency of the driver is affected by any impedance mismatch. On the other hand, at the terminals of a pickup the output voltage (V_p) and power at the unmatched load *do* depend on the loading.

Maximum power is delivered from a pickup when a matched load lowers Q_L by one-half to $Q_U/2$; this is the condition assumed in the Eqs. 4.17 and 4.19 for the transfer impedance, and Eqs. 4.21 and 4.22 for signal output power. For other degrees of loading,

TABLE I

Longitudinal	Transverse
Kickers	
$V = K_{\|\|}\, V_K$	$\Delta p_\perp \beta c / e = K_\perp\, V_K$
	$K_\perp = -\frac{1}{jk} \nabla_\perp K'_{\|\|}$.
$P_K \equiv \|V\|^2 / 2R_{\|\|} T^2$	$P'_K \equiv \|\Delta p_\perp \beta c / e\|^2 / 2R_\perp T^2$
$R_{\|\|} T^2 = Z_c \|K_{\|\|}\|^2$	$R_\perp T^2 = Z_c \|K_\perp\|^2$
Relations Between Pickups and Kickers	
$Z_p = \frac{1}{2} Z_c\, K_{\|\|}$	$Z'_p = -\frac{1}{2} jkZ_c K_\perp$
$Z_p = \sqrt{Z_c\, R_{\|\|}\, T^2/2}$	$Z'_p = k_B \sqrt{Z_c\, R_\perp\, T^2/2}$
Pickups	
$Z_P \equiv V_p / I_B$	$Z_{P'} \equiv V_{P'} / I_B\, \Delta x$
$P_p = \langle I_B^2 \rangle R_{\|\|}\, T^2/4$	$P'_p = \langle I_B^2\, x^2 \rangle k_B^2\, R_\perp\, T^2/4$

[a]As noted in Appendix 1, some authors define the transverse beam voltage as simply $c\Delta p_\perp$, omitting the factor of β. Using this convention, one would simply need to replace all the k_B appearing in the above formulas by the free-space wave-number $k = \omega/c$. The effect of this change will be to re-define the transverse kicker constant and shunt impedance, but to leave the calculated physical quantities of input power and transverse momentum kick unchanged.

it is straightforward to show that the pickup signal power is reduced by a factor of $4Q_L(Q_U - Q_L)/Q_U^2$. The result for the transfer impedance is slightly more complicated, as it depends on the origin of the mismatch. The cavity signal is usually coupled out via an antenna or loop which serves as an impedance transformer. The mismatch can be due either to attaching the wrong load, or incorrectly adjusting the coupling for the correct load. In the former case, one compares the values of Z_p with the same coupling but different loads; in the latter, the same load but different couplings. As with the case of the power, the results can be expressed in terms of Q_U and Q_L.

$$Z_p^{wrong\ Z_L} = \frac{2\,Q_L}{Q_U}\, Z_p^* \tag{4.25a}$$

$$Z_p^{wrong\ m} = \frac{2\,Q_L}{Q_U} \sqrt{\frac{Q_U - Q_L}{Q_L}}\, Z_p^* \tag{4.25b}$$

5. Beam Impedance; A Simple Model

Strictly speaking, the notion of beam impedance need not be introduced into a discussion of pickups and kickers. However, doing so serves several pedagogical purposes. The primary purpose is to provide a simple physical picture for the beam impedance which also serves as a simple model for the shunt impedance, and hopefully serves somewhat to demystify both these concepts. It also provides a demonstration of the power and utility of both the Panofsky-Wenzel theorem and the concept of beam voltage. Discussion of the model also provides a natural way to introduce the notion of image charges and currents.

Let us consider a charged particle moving in a conducting enclosure, such as a beam tube. The electric field lines emanating from the charge terminate on the walls, where a charge density proportional to the field is induced. For highly relativistic particles, the field lines are foreshortened in the longitudinal direction so that they are very nearly perpendicular to the direction of motion, forming what is essentially a two-dimensional field. Hence the charges on the wall appear at the same longitudinal position as the beam particle and move along with it, forming an annular "image" of the beam. For a beam centered on the axis of a circular beam tube, the image charges will exhibit azimuthal symmetry.

The notion of beam impedance arises from the fact that when a particle beam moves through any portion of an accelerator, it generates electromagnetic fields, primarily due to its image charges and currents, which then act back on the beam, causing it to lose energy and/or undergo a transverse deflection. Considering the former case, a reasonable characterization of this self-interaction would be the ratio of the particle energy loss (expressed as a voltage) divided by the current, in other words, an *impedance*; it is this quantity which is defined as the longitudinal *beam impedance*. (In like fashion one can define a transverse beam impedance.)

If we now recall the case of a pickup, we realize that the output power derived from such a device must come from the work done by the beam against the fields which it *itself* generates. Moreover, these fields are precisely those which produce the energy loss appearing in the definition of the beam impedance. Hence, it should come as no great surprise that the beam impedance turns out to be directly proportional to the shunt impedance. The actual factor relating the two impedances is device-dependent; however for many devices, Z^{beam} is simply $RT^2/2$, i.e. the device shunt impedance in parallel with its (equal) matched load.

The notion of beam impedance is clearly more general than shunt impedance, since it applies equally well to devices with *no* external connections, for which devices the notions of shunt impedance and transfer impedance would be meaningless. Moreover, as defined in terms of power efficiency, the shunt impedance is intrinsically a real quantity, i.e. it contains no phase information; the beam impedance, defined in terms of voltage, *can* contain such information. However, in the examples given below, we shall assume it to be a purely real quantity.

a. Longitudinal Beam Impedance

The models we will use to describe longitudinal impedance are assumed to be one dimensional, i.e. the fields associated with them are assumed to be plane "waves" which exhibit only longitudinal variation. Let us imagine that we have a device located in some portion of the beam tube; such a "device" could be a pickup electrode, an rf cavity, or even the wall of the beam tube itself. If we characterize such a device (or equivalently, its impedance) as a simple resistance, as shown in the figure below, then any voltage im-

pressed on that resistance, either induced by the beam or resulting from an external voltage source, will be assumed to produce a uniform longitudinal electric field in the region between points a and b (and no field anywhere else).[4]

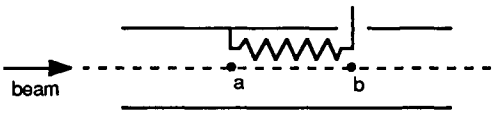

Fig. 5 Schematic representation of a beam impedance

On what basis is this model plausible? Recall our discussion of the beam voltage in Sect. 2. It was pointed out there that if one knows the beam voltage V, one knows it all: The value of V gives the energy change in the beam, and (by Panofsky-Wenzel) its transverse derivative gives the transverse momentum kick it receives. It was further pointed out that the boundary condition for that (two-dimensional) field was simply the voltage change at the wall of the beam tube. What we are doing then, is contriving a simple mechanistic (electristic?) model for the generation of V. On pedagogical grounds, we have made the model somewhat simplistic: We assume that the impedance is a resistance, and we idealize the transverse behavior of the beam voltage by asserting that it is uniform across the beam tube. (The latter assumption will be replaced by an equally simplistic model when we discuss transverse effects.)

The creation of such a field by an externally applied voltage is easily understood. An equally simple model can be constructed for the creation of the beam-induced field. When a beam current I_B passes inside the beam tube, an equal and opposite beam-induced current flows on the wall of the beam tube. At the point at which the wall current is intercepted by the resistance R, it will produce a voltage across R given by $V_R = -I_B R$.[5]

Having made that simple statement, it is necessary to qualify it immediately. Recalling that the beam is actually a sinusoidally varying current $I_B \exp[j(\omega t - kz)]$, the instantaneous voltage across R at any instant is actually

$$V_R(t) = \frac{R}{b-a} \int_a^b I_B \, e^{j(\omega t - kz)} \, dz \tag{5.1}$$

Evaluating the above integral, we see that V_R is still a sinusoid, but with a maximum value of the form

$$|V_R| = I_B R \, \frac{\sin \theta}{\theta} \tag{5.2}$$

where $\theta = k(b-a)/2$. We immediately recognize the $\sin\theta/\theta$ term as the transit- time factor T for a uniform field (see Appendix 2); in this case, its appearance results from the

[4]Clearly a resistance located on one side of the accelerator beam tube, as shown in the figure, could not produce such a one-dimensional field, and so the model is to be understood as a schematic representation of an azimuthally uniformly distributed resistance. In addition, we have further simplified our one-dimensional model by neglecting end effects, i.e. assuming the field to be uniform between a and b.

[5]In our model, we assume that the entire image current flows throught R_s. The device modelled by R_s may not actually intercept all the image current; in fact, as we shall see in the case of devices such as capacitive pickups and striplines, the value of R_s may reflect this fractional interception of the beam.

spatial sinusoidal variation of the current. However, when a particle experiences a self-field due to the presence of an impedance, the factor T enters *twice*: once in the voltage generated across the impedance, and a second time as a reduction of the effective field experienced by the beam.

b. Resonant Cavity/Resistive Wall Monitor

There are a number of devices whose impedance in an equivalent circuit may be modelled as a pure resistance; among these are resistive wall monitors and cavities at resonance. The former are constructed of (an azimuthally symmetric array of) resistors mounted in the wall of the beam tube–and looking suspiciously like the simple model we have been discussing–and theirs is a broad band impedance; the latter are resistive only at resonance, and hence are narrow band.

We now assert, and will shortly provide a hand-waving demonstration, that a cavity *also* behaves as though *its* shunt impedance were similarly located in the beam tube wall; we further assert that when either type of device is connected to an external electric circuit, it behaves as though its electrical impedance were identical with its shunt impedance. A consequence of the latter result is that for such a device to behave as a matched source/load, it must be connected to the external circuit via an impedance matching device such as a transformer. The equivalent circuit for such a model is shown in Fig. 6. Note that the transformer in this model (and in all subsequent models) is assumed to be ideal, i.e. the only impedance it presents is the appropriately transformed impedance of the loads connected to it.

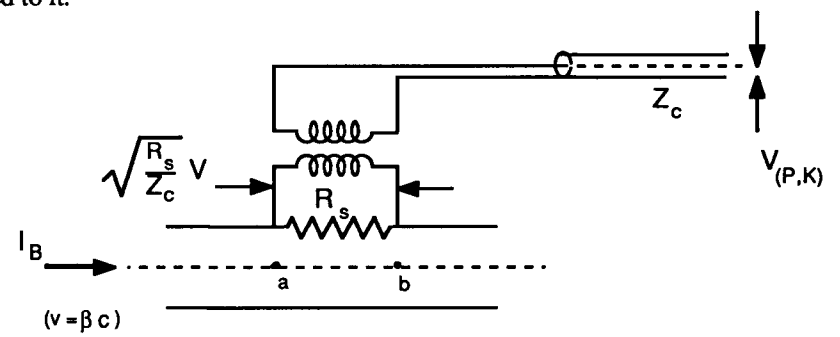

Fig. 6 Schematic representation of resistive impedance including matched input/output to permit use as a pickup/kicker.

We will now show that, *if the value of R_s is taken to be that of the device's* cavity *shunt impedance*,[6] the model yields the correct result for the longitudinal shunt impedance and kicker constant when the device is considered as a kicker, and for the transfer impedance and signal output power, when the device acts as a pickup. Finally we will use the model to obtain the beam impedance of the device.

i. Kicker Performance Predicted by Model. The input power to the kicker shown above is simply

$$P_K = V_K^2/2Z_c \tag{5.3}$$

If our model gives a valid representation for R_s, then according to Eq. 4.9, P_K should be

[6]That is, the the shunt impedance *sans* transit-time factor.

equal to $\langle(\Delta E/e)^2\rangle/R_s T^2$. From the model, we see that the peak voltage appearing across the wall resistor is $\sqrt{R_s / Z_c} V_K$; because of the transit-time effect, the peak energy change imparted to the beam is

$$V = \sqrt{\frac{R_s}{Z_c}} V_K T \tag{5.4}$$

From Eq. 4.1, we see that the kicker constant is then given by

$$K_{\|} = \sqrt{R_s T^2 / Z_c} \tag{5.5}$$

in agreement with Eq. 4.10. Squaring Eq. 5.4, dividing both sides by $R_s T^2$, and taking expectation values, we have

$$\frac{\frac{1}{2}\left|V^2\right|}{R_s T^2} = \frac{\frac{R_s}{Z_c}\frac{1}{2}\left|V_K{}^2\right| T^2}{R_s T^2} = \frac{\left|V_K{}^2\right|}{2 Z_c} \qquad \text{Q.E.D.} \tag{5.6}$$

ii. Pickup Performance Predicted by Model. We now wish to see if the model predicts the correct output power and transfer impedance. Assuming that the external load is correctly matched, our model predicts that the peak voltage developed across R_s due to a (peak) beam current I_B is

$$V_R = I_B R_s T/2 \tag{5.7}$$

This leads to an output voltage

$$V_p = \frac{I_B R_s T}{2} \sqrt{\frac{Z_c}{R_s}} \tag{5.8}$$

which in turn gives a transfer impedance of

$$Z_P = \sqrt{Z_c R_s T^2}/2 \tag{5.9}$$

in agreement with Eq. 4.23. From Eq. 5.8 we can also calculate the output power

$$P_P = \left\langle \left(\frac{I_B R_s T}{2}\sqrt{\frac{Z_c}{R_s}}\right)^2 \right\rangle \cdot \frac{1}{Z_c} = \frac{\left\langle (I_B)^2 \right\rangle R_s T^2}{4} \tag{5.10}$$

in agreement with Eq. 4.21.

It should now be apparent where the extra factor of 1/4 in Eq. 4.21 (relative to Eq. 4.9) comes from. In the case of the kicker, we compared the (square of the) beam voltage gain to the power into the kicker (i.e. neglecting any power dissipated in the power supply's internal impedance). In the case of the pickup, firstly the existence of a matched external load decreases the device's apparent impedance (and hence the total power dissipated by a given current) by half; secondly, half of that reduced power is dissipated in the impedance of the device itself, so that only 1/4 of the power which would have been dissipated in the unloaded device itself is available to the external matched load. Similar considerations will be seen to apply to Eq. 4.22 for the transverse case.

iii. Beam Impedance We have now seen that the longitudinal interaction with the beam of a cavity at resonance or a resistive wall can be modelled as a series resistance equal to the device's longitudinal shunt impedance. It now remains to calculate the beam impedance of such a device.

Using the expression in Eq. 5.7 for the voltage induced by the beam in the wall impedance, and recalling that an additional factor of T appears in the voltage which acts back on the beam, we see that the amplitude of the beam voltage is just $(-)I_B R_s T^2/2$. Hence the longitudinal beam impedance, which is just the (negative of the) ratio of beam self-voltage to beam current is given by

$$Z_{\|} = R_s T^2/2 \tag{5.11}$$

Note that if the device were *un*loaded, the beam impedance would simply be equal to the shunt impedance (using our convention that that impedance includes the square of the transit-time factor). It might appear that this is a universal result, i.e. true for any device whose shunt impedance is resistive; however we shall see in the following section that this is not the case.

c. Transverse Impedance

The model we will be using for transverse impedance is similar to that for longitudinal impedance, but will of necessity involve two-dimensional, rather than one-dimensional fields, i.e. the fields must exhibit transverse variation. A simplified model for a transverse impedance (such as a pickup) is shown below; as with the longitudinal case, the same model will apply for a transverse kicker as well. However, we begin by considering its impedance/pickup behavior, i.e. its response to a beam.

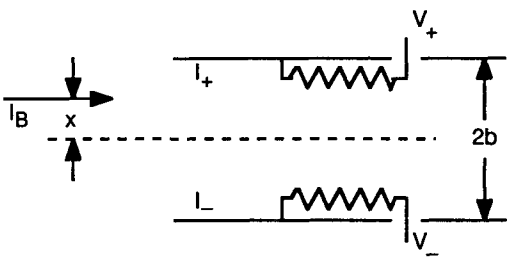

Fig. 7 Schematic representation of a transverse beam impedance

The image currents produced by the beam will divide between the two resistances; in contrast to the longitudinal impedance, if the beam is displaced from the centerline of the device, the currents will divide *unequally*. Throughout the discussion, we will assume that this division varies *linearly* with the beam displacement, i.e.

$$I_+ = (I_B/2) \cdot (1 + x/b) \tag{5.12a}$$

$$I_- = (I_B/2) \cdot (1 - x/b) \tag{5.12b}$$

Note that if such a device is actually used as a pickup, the difference of the output voltages V_+ and V_ will be proportional to $I_B x$, the desired output for a transverse pickup.

To use the model to describe kicker behavior, one assumes equal but opposite voltages $\pm V_R$ to be induced across the two resistors. Using the same linear approximation, one further assumes that the longitudinal beam voltage in the region between the resistors varies as

$$V(x) = V_R \cdot x/b \; (\cdot T) \tag{5.13}$$

Since the longitudinal kicker constant is directly proportional to the longitudinal beam voltage, and $\nabla_\perp V(x) = \partial V/\partial x = V_R/b$, we have from Eq. 4.7[7]

$$K_\perp = -\frac{1}{j k_B} \nabla_\perp K_\parallel'(x) = -\frac{1}{j k_B b} K_\parallel'(b) = -\frac{1}{j k_B b} \sqrt{\frac{R_s T^2}{Z_c}} \tag{5.14}$$

Again, we have used the notation $K_\parallel'$ in Eq. 5.14 to emphasize the fact that the longitudinal kicker constant referred to is the one associated with the excitation mode for which one wishes to calculate $K_\perp$. As we shall see, for many "devices" (e.g. resistive walls), the same resistance can be used to characterize both the longitudinal and transverse impedances; in such a case $K_\parallel'(b)$ will have the same value as $K_\parallel$ for the longitudinal mode. For devices such as striplines, we shall see that this is a reasonable approximation; on the other hand, for devices such as resonant cavities, the transverse excitations not only are almost always associated with impedances different from the longitudinal ones, but occur at different frequencies.

We can now use Eq. 5.14 in conjunction with Eqs. 4.10, 4.11 and 4.23, 4.24 to obtain the following simple relations between the shunt impedances and transfer impedances

$$R_\perp T^2 = R_\parallel(b)\, T^2 \left(\frac{\lambda_B}{b}\right)^2 \tag{5.15}$$

$$Z_P' = Z_P(b)/b \tag{5.16}$$

where in Eq. 5.15 we have dispensed with the "prime" notation, and restored it to its original meaning in Eq. 5.16. As was the case with Eq. 5.14, for those devices for which the same resistors can be used to model longitudinal and transverse impedance, the longitudinal impedances in Eqs. 5.15 and 5.16 can be replaced with those corresponding to the longitudinal excitation mode.

One final note: For a device such as a resonant cavity, the individual resistances have no physical significance, so there is no actual differencing of two signals (the model simply says that the cavity "behaves as if" it were taking such a difference). On the other hand, for devices such as resistive wall monitors and striplines, one *can* get separate output voltages. For such devices, the sum of the output voltages V_+ and V_- will be proportional to the total current I_B, whereas the difference signal will be proportional to $I_B x$; in other words, depending upon how one combines the output signals for such a device, it can be used as either a longitudinal or a transverse pickup.[8]

[7] It is perhaps worth repeating yet once more the importance of the Panofsky-Wenzel theorem. By implicitly taking into account the electromagnetic relation between the longitudinal fields and the transverse deflecting fields, it has made it possible for us to explain transverse electromagnetic effects using a longitudinal, low-frequency ac–actually a time-varying dc–model (plus transit-time effects).

[8] In fact, if a 180° hybrid is used to combine the signals, it can provide *both* sum *and* difference outputs, thereby enabling the device to act as both a longitudinal and a transverse pickup simultaneously.

d. Resonant Cavity/ Resistive Wall

The model for a transverse resistive impedance is shown in Fig. 8. As discussed in the preceding section, the value of the R_s used in modelling the transverse impedance may, in the case of an actual resistance, be the same as that for the longitudinal impedance,[9] and the combiner element will be a piece of actual hardware; in the case of a cavity, the value of R_s will almost certainly be different from the longitudinal value, and the combiner element is symbolic. As was the case for the longitudinal model discussed earlier, an ideal transformer is included for purposes of impedance matching.

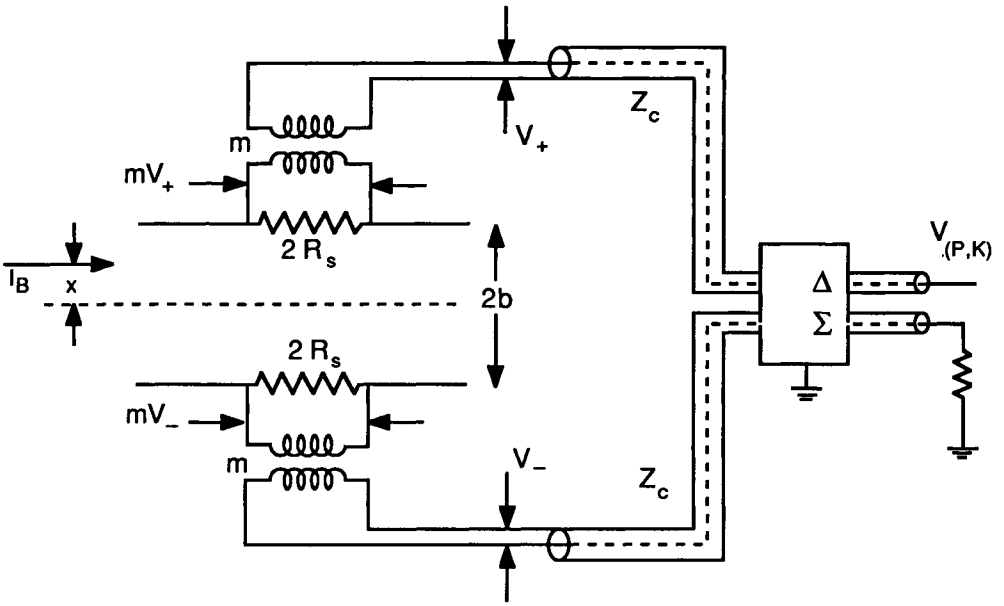

Fig. 8 Schematic representation of transverse resistive impedance including matched input/output to permit use as a pickup/kicker.

i. Kicker Performance Predicted by Model As with the longitudinal case, the input kicker power is given by

$$P_K = V_K^2/2Z_c \tag{5.17}$$

Assuming a matched combiner, V_+ will be $V_K/\sqrt{2}$. For proper impedance matching, m will be equal to $\sqrt{2R_s/Z_c}$, so that the transverse kick will be given by

$$\frac{\Delta p_\perp \beta c}{e} = -\frac{1}{jk}\frac{\partial V_B}{\partial x} = -\frac{1}{jk}\sqrt{\frac{R_s}{Z_c}}\frac{V_K T}{b} \tag{5.18}$$

Substituting Eqs. 5.17 and 5.18 into the definition of $R_\perp T^2$ (Eq. 4.11) gives

[9]With the original resistance split into two parallel branches, each branch has resistance $2R_s$.

$$R_\perp T^2 = \frac{\left(\Delta p_\perp \beta c / e\right)^2}{V_K^2 / Z_c} = \frac{R_s}{Z_c}\frac{V_K^2 T^2}{k_B^2 b^2}\frac{Z_c}{V_K^2}$$

$$= \frac{R_s T^2}{k_B^2 b^2} = R_s T^2 \left(\lambda\!\!\!^{-}_B / b\right)^2 \tag{5.19}$$

Equation 5.19 is susceptible to two interpretations. The most straightforward one is to to regard the transverse and longitudinal models as independent (as they are, say, for cavities), and regard Eq. 5.19 as defining the value of R_s required to give the correct transverse shunt impedance. On the other hand, for devices for which the same R_s can represent both the longitudinal and transverse impedances, Eq. 5.19 says that the transverse *shunt* impedance is the obtained by simply multiplying the longitudinal shunt impedance by a factor of $(\lambda\!\!\!^{-}/b)^2$. Note that under either interpretation, if we assume R_s to be frequency-independent, then Eq. 5.19 says that the device's efficacy as a transverse kicker falls off with increasing frequency, consistent with the observations made earlier in Sect. 1b when discussing the Panofsky-Wenzel theorem. In fact, as we shall see, the factor is present in the expression for transverse shunt impedance for a wide variety of devices.

ii. Pickup Performance Predicted by Model From Fig. 8, we see that with the external matched load paralleling the device impedance, each resistor present to the beam an impedance of R_s. Denoting, as per Fig. 7, the upper and lower currents as $I^\pm$, we have for the voltages across the respective resistances $I^\pm R_s T$, and for the voltages in the respective output lines

$$V_\pm = \sqrt{Z_c / 2R_s}\, I^\pm R_s T = I^\pm \sqrt{Z_c R_s / 2}\, T \tag{5.20}$$

whereby, using the linear approximation in Eqs. 5.12a,b for $I^\pm$, the voltage out of the (differencing) signal port is given by

$$V_P = \frac{1}{\sqrt{2}}\sqrt{Z_c R_s / 2}\, T\left(I^+ - I^+\right) = \frac{I_B x}{2b}\sqrt{Z_c R_s}\, T \tag{5.21}$$

Hence the power output into a matched load of impedance Z_c is

$$P_P = \left\langle (I_B x)^2 \right\rangle \frac{R_s T^2}{4b^2} = \left\langle (I_B x)^2 \right\rangle \frac{R_\perp T^2}{4\lambda\!\!\!^{-2}} \tag{5.22}$$

which is just the expected result; in other words, the value of R_s which gives the correct transverse kicker shunt impedance properly predicts the transverse pickup performance.

iii. Beam Impedance The standard definition for transverse beam impedance is

$$Z_\perp \equiv j \frac{\Delta p_\perp c / e}{I_B x_B} \tag{5.23}$$

where $\Delta p_\perp$ is the transverse kick due to to the fields generated by the beam itself, and x_B is the transverse position of the beam. To calculate $\Delta p_\perp$ we need to know the self-induced

beam voltage at the position of the beam. From Eqs. 5.12a,b we see that the beam induces across the two resistances equal and opposite voltages of

$$mV^{\pm} = I_B x_B R_s T/(2b) \tag{5.24}$$

(There is also a "sum" voltage" equal to $I_B R_s T$; because this produces a beam voltage with no transverse gradient, it is of no interest in calculating $\Delta p_\perp$.) From Eq. 5.13, we see that the voltages in 5.24 give rise to a beam voltage[10]

$$V = -\frac{I_B x_B R_s T}{2b}\frac{x}{b}T = -\frac{I_B x_B\, x\, R_s T^2}{2b^2} \tag{5.25}$$

Applying the Panofsky-Wenzel theorem gives

$$\Delta p_\perp = -\frac{1}{j\omega}\frac{\partial V}{\partial x} = -\frac{1}{j\omega}\frac{I_B x_B R_s T^2}{2b^2} \tag{5.26}$$

Inserting this expression into Eq. 5.23 gives

$$Z_\perp = \frac{1}{k_o}\frac{R_s T^2}{2b^2} \tag{5.27}$$

where $k_o = \omega/c$ is the free-space wave number. Comparison with Eq. 5.18 shows that

$$Z_\perp = \frac{1}{2} R_\perp T^2 \frac{\lambda\!\!\!^{-}_o}{\lambda\!\!\!^{-2}_B} \tag{5.28}$$

As with the longitudinal beam impedance, the factor of 1/2 is due to the presence of the (equal) external load. Note that had the factor of β been included in the definition of $Z_\perp$, as it is in the definition of the transverse beam voltage, the right hand side of Eq. 5.27 would have simplified to $R_\perp T^2/2\lambda\!\!\!^{-}_B$. Similarly, were we to compare with the alternate definition of transverse shunt impedance $R_\perp T^2 \cdot k_o$(see the discussion following Eq. 4.11) which we will define as $R_\perp{}^{\text{alt}}$, we see that

$$Z_\perp = \frac{1}{2} R_\perp^{alt} \frac{\lambda\!\!\!^{-2}_o}{\lambda\!\!\!^{-2}_B} \tag{5.29}$$

i.e. with a consistent convention regarding the inclusion of β (or in the limit of $\beta \to 1$), $Z_\perp$ for the unloaded device would be the same as $R_\perp{}^{\text{alt}}$.

Two final notes: For devices such as resistive walls, where the same R_s applies in both longitudinal and transverse cases, we can use Eq. 5.11 to rewrite Eq. 5.28 to a form which may be familiar to those having some background in accelerator design

$$Z_\perp = \frac{1}{k_o b^2} Z_\parallel = \frac{1}{k_o^{rev} b^2}\frac{Z_\parallel}{n} \tag{5.30}$$

[10]Note the presence of both an x and an x_B term, since this is the beam voltage at any position due to a beam at x_B.

where k_o^{rev} is the wave number associated with the particle revolution frequency, and n is the revolution harmonic number corresponding to the frequency of interest; the "1" in the numerator results from the assumed one-dimensional nature of the transverse field. Secondly, the use of *two* resistors has been necessary for modelling transverse kickers and pickups and relating them to beam impedance, and also simplified the discussion of the latter quantity. However, for transverse beam impedance alone, a single resistance, distributed azimuthally as postulated in conjunction with the longitudinal model, would have sufficed; a transverse self-voltage would have resulted from the non-uniform distribution of the image currents in the distributed resistor. Because the resulting beam voltage distribution would have been two-dimensional, as well as for the other pedagogical reasons cited, we elected to stay with the two-resistor model throughout the discussion.

C. PROPERTIES OF SPECIFIC DEVICES

Pickups and kickers comprise a wide panoply of electromagnetic devices. The choice of a given device for a particular application will depend on such things as the required strength of coupling to the beam (i.e. the shunt impedance), bandwidth, and overall length (which may be constrained by the amount of available "real estate" in the accelerator). As we shall see, the choice of a particular type of device will entail a trade-off of these quantities against one another, and so the requirements of the application will strongly influence that choice. For example, r-f acceleration requires high power, i.e. efficient coupling, but can be accomplished using a single frequency, i.e., narrow bandwidth. On the other hand, for beam sensors where a large number of devices is desirable, especially for compact rings, smallness in size may be a driving consideration. Moreover, due to the large peak currents in many electron machines, not only may the beam sensors in such machines have weaker coupling, but because beam impedance is closely related to shunt impedance, having many sensors with strong coupling may be positively undesirable.

In the sections which follow we will examine a variety of electrodes that are used as pickups and kickers. We will describe their basic operation principles, and obtain expressions for their coupling parameters,in many cases giving numerical values for these parameters, and mention typical applications. Equally important from the point of view of these notes, these derivations will illustrate the application of the results of the first part of this report to calculating properties of actual devices.

6. The Resonant Cavity

Conceptually, one of the simplest electrode systems is the cavity resonator; for simple shapes its fields are easy to visualize and are approximately calculable in closed form, so that its response (within its resonant bandwidth) is readily predictable. Because of its very efficient coupling to the beam, it finds widespread use. One of its most common applications is as the source of the accelerating r-f voltage, in which it acts as a longitudinal kicker. It is well suited for detecting or controlling by feedback particular modes (i.e., modes at a particular frequency) of beam instability. As a pickup, it finds application in situations where the beam signals are weak, as was the case for the Schottky signals shown in Sect. 3c.

In its function as an accelerating structure, the cavity is excited in its lowest TM mode, producing nearly uniform longitudinal electric fields, at least in the region traversed by the beam. To function as a transverse kicker, it must be excited in a higher order TM mode[11]

[11]Recall from the Panofsky-Wenzel theorem that a transverse kicker requires a *longitudinal* electric field.

which, while again usually uniform in the longitudinal direction, exhibits a transverse gradient at the beam location. Used as a pickup it will respond to transverse beam signals at the frequencies corresponding to those modes at which it can act as a transverse kicker.

a. Longitudinal Kicker/Pickup

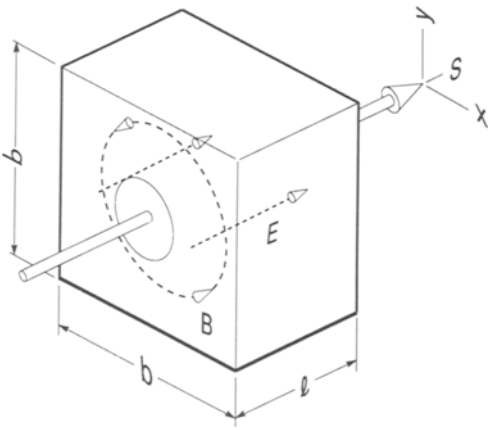

Fig. 9. Fields in longitudinal cavity-electrode.

Let us begin by considering the square cavity shown in Fig. 9. From reciprocity we know we need only calculate its performance as either a pickup or a kicker. It turns out that the latter is by far the simpler, particularly if we assume that for moderately sized beam-tube apertures the cavity can be treated as a closed rectangular box. In particular, if we go back to Eq. 4.9, the defining relation for the kicker shunt impedance, we find that all the terms are calculable in closed form. Using the conventional expression for the energy input to a cavity at resonance, we may rewrite Eq. 4.9 as

$$R_{\|}T^2 = \frac{V^2}{2P} = \frac{1}{2}\frac{V^2}{\omega_r U/Q_U} \tag{6.1}$$

where Q_U is the Q-value for the unloaded cavity, ω_r is the resonant frequency, U is the stored energy within the cavity, given by

$$U = \frac{1}{2}\varepsilon_o \int_{vol} \mathbf{E}^2 \, d\,vol \ . \tag{6.2}$$

and V, the beam voltage is given by the (by now, hopefully, familiar) expression

$$V = \int e^{jkz} E_z dz \tag{6.3}$$

The lowest cavity mode with maximum longitudinal electric field along the centerline is mode TM_{110}, for which the wavelength is $\lambda = \sqrt{2}\, b$ and the electric field is

$$\mathbf{E} = E_z = E_o \cos\frac{\pi x}{b} \cos\frac{\pi y}{b} \tag{6.4}$$

uniform in the z-direction. Inserting this into Eq. 6.3 at $x = y = 0$ gives

$$V = E_o \ell \frac{\sin\theta}{\theta} \equiv E_o \ell T \tag{6.5}$$

where we again see the familiar transit time factor, with $\theta = \omega_r \ell/2v = k_O \ell/2\beta$. From Eq. 6.4. we find

$$U = \frac{1}{8} \varepsilon_o E_o^2 \ell b^2 \tag{6.6}$$

(Eq. 6.6 holds for *any* TM_{mn0} mode; however, only those with both m and n odd are useful for a longitudinal kicker.) Substituting in Eq. 6.1 we obtain

$$R_{\|}T^2 = \frac{4}{\pi} Z_o \frac{\ell}{\lambda} QT^2 = 480 \frac{\ell}{\lambda} QT^2 \text{ ohm} \tag{6.7}$$

where $Z_O = (\varepsilon_o c)^{-1} = 1/\sqrt{\varepsilon_o/\mu_o}$ is the impedance of free space (sometimes denoted in electrical engineering texts by η). We can generalize this to the case of an arbitrary TM_{mno} mode by replacing $\lambda = \sqrt{2}\, b$ with

$$\lambda = 2b/\sqrt{m^2 + n^2} \tag{6.8}$$

whereby Eq. 6.7 becomes

$$R_{\|}T^2 = \frac{8}{\pi} \frac{\ell}{\lambda} \frac{Z_o QT^2}{m^2 + n^2} = \frac{960}{m^2 + n^2} \frac{\ell}{\lambda} QT^2 \text{ ohm} \tag{6.9}$$

As an example of another shape, for a circular-cylinder (pillbox) cavity, we find that the shunt impedance for the lowest longitudinal TM mode (TM_{010}) is given by

$$R_{\|}T^2 = \frac{2}{[\rho_{01} J_0(\rho_{01})]^2} \mu_o c \frac{\ell}{\lambda} QT^2 \tag{6.10}$$

in which ρ_{01} (the first zero of $J_O(x)$)= 2.405 giving

$$R_{\|}T^2 = 484 \frac{\ell}{\lambda} QT^2 \tag{6.11}$$

a result nearly identical with that for the square cavity

Using ℓ-dependence of Q_U for a closed box cavity, we find that a broad maximum value of the quantity $\ell QT^2/\lambda$ occurs for $\beta=1$ at $\theta = 1.37$ radian at which $\ell/\lambda = 0.44$ and $T^2 = 0.51$. At that optimum length, the simple cavity then gives

$$R_{\|}T^2 \approx 108\, Q \text{ ohm} \ . \tag{6.12}$$

By modifying the cavity shape (e.g., reducing the longitudinal gap in the region immediately surrounding the beam tube), this figure may be increased, principally due to increasing the transit-time factor, by about 25%. In these equations, the *unloaded* quality factor Q_U is used. Values for this quantity (for a non-superconducting cavity) may be as high as 30,000 at 1 GHz, and exhibit a frequency variation of $\sqrt{1/\omega}$.

One must be able to couple power in or out of the cavity (depending on whether it is used as a kicker or a pickup), usually done using a loop or stub antenna (represented schematically by a transformer in Sect. 5). For maximum efficiency, one uses matched coupling, thereby reducing the Q of the circuit by a factor of 2. As discussed in Sect. 4, under this matched condition, the power out of a longitudinal cavity pickup will still be given by Eq. 4.21, where one is to use the *unloaded* Q in the expression for $R_{\|}T^2$. (The response width of the cavity will of course be given by the *loaded* Q, i.e. $\Delta\omega/\omega = 2/\text{Q}$.)

Similarly the transfer impedance for a matched cavity is given by Eq. Eq. 4.23, where again, one uses the unloaded Q in calculating $R_{\|}T^2$. Assuming a standard output impedance of $Z_c = 50\ \Omega$, the transfer impedance will be given by

$$Z_P = 37\sqrt{Q} \text{ ohms} \tag{6.13}$$

The effect of impedance mismatch has been described in Sect. 4c.

b. Transverse Kicker/Pickup

As with the longitudinal cavity, we begin with the definition of shunt impedance, given in this case by Eq. 4.11. Inserting the expression for cavity power and using the Panofsky-Wenzel theorem, we obtain

$$R_{\perp}T^2 = \frac{(\Delta p \beta c/e)^2}{2P} = \left(\frac{1}{k_B}\frac{\partial V}{\partial x}\right)^2 \frac{Q_U}{2\omega_r U} \tag{6.14}$$

where again U and V are given by Eqs. 6.2 and 6.3.

The lowest order on-axis x-deflecting mode is the the TM_{210}; the wavelength is again given by Eq. 6.8, which for this mode takes the value $2b/\sqrt{5}$, and the electric field is

$$\mathbf{E} = E_z = E_o \sin\frac{2\pi x}{b}\cos\frac{\pi y}{b} b^2 \tag{6.15}$$

Proceeding as with the longitudinal cavity, we obtain the result

$$R_{\perp}T^2 = \frac{32}{25\pi} Z_o \beta^2 \frac{\ell}{\lambda} QT^2 = 154\, \beta^2 \frac{\ell}{\lambda} QT^2 \tag{6.16}$$

where T has the same definition as in Eqs. (6.5). For the general TM_{mn0} mode (for an x-deflecting kicker, m must be even, and n odd) this becomes

$$R_\perp T^2 = \frac{8}{\pi}\frac{\ell}{\lambda}\frac{Z_o \beta^2}{m^2+n^2}\frac{m^2}{m^2+n^2}QT^2 = 960\,\beta^2\frac{\ell}{\lambda}\frac{m^2}{(m^2+n^2)^2}QT^2 \qquad (6.17)$$

For the TM_{210} mode (and $\beta \approx 1$), maximum $\ell QT^2/\lambda$ occurs at $\theta = 1.41$, for which value

$$R_\perp T^2 = 33.7\ Q\ \Omega. \qquad (6.18)$$

If the cavity is used as a transverse pickup, assuming its output is matched into a 50 Ω output impedance, Eq. 4.24 gives for the transfer impedance

$$Z_P' = 20.5\, k_o\sqrt{Q}\ \ \Omega/\text{m} \qquad (6.19)$$

It was a cavity such as this[17] that was used to obtain the Schottky spectrum shown in Sect. 3. The cavity, nominally 15 cm on each side, was machined of aluminum and had the following properties

$$f = 2.045\ \text{GHz}$$
$$\frac{R_\perp T^2}{Q} = 29\ \Omega$$
$$Q_U = 9500$$
$$Z_P' = 81 \times 10^3\ \Omega/\text{m}$$

The reduced R/Q (relative to that predicted by Eq. 6.21) is probably due to the fact that the operating frequency was sufficiently close to the aperture cut-off frequency (≈2.5 GHz) that the penetration of the fields into the beam tube made the closed-box model of the cavity only approximate.

7. The Capacitive Pickup

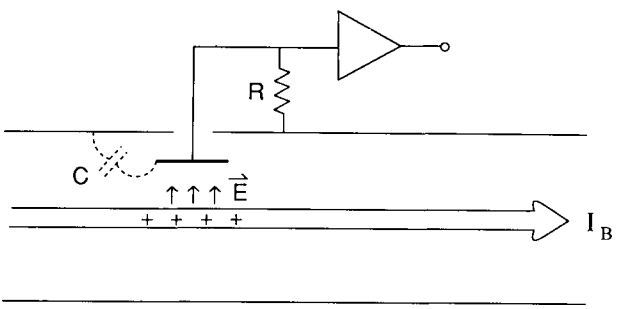

Fig. 10. Schematic Representation of Single-Plate Capacitive Pickup

We now consider the behavior of the device we have been using as the illustrative model of a pickup/kicker electrode, the isolated plate(s) in the wall of the beam tube. For simplicity we begin our treatment using a single-plate, as shown schematically in Fig. 10.

Because such a device behaves essentially as a pure capacitance, it cannot act as a matched load; hence, in its "pure form" it is of limited utility as a kicker. One way around this limitation is to "resonate" the capacitor using a parallel inductance, resulting in a device, like the cavity, which has a high, resistive, shunt impedance over a relatively narrow bandwidth; we will discuss this technique later in this section The other is to lengthen the plate so that it becomes a transmission line, or stripline, with a characteristic impedance; this approach will be discussed in the following section.

For a variety of reasons, it is useful to analyze the capacitive pickup using image currents, rather than by treating it as a kicker and using reciprocity. First, the reciprocity approach is complicated by the impedance mismatch. Second, for those problems for which the image-current approach is applicable, situations in which the device is short compared to the beam wavelength, one can generally employ an intuitive approach to solving them. Finally, the image-current approach is pedagogically useful in illustrating some of the complementary aspects of the time- and frequency-domain pictures.

If we imagine the pickup plate in Fig. 10 to be of length ℓ, then the image-current analysis will be valid at frequencies for which $\hat{\lambda} > \ell$. Recall from our discussion of beam spectra from Sect. 3, that for a machine with every bucket filled, the lowest frequency (strong) line in the coherent spectrum is that of the rf itself. Hence the above requirement is equivalent to saying that if we wish to observe the beam at the rf frequency, the pickup must be short compared to the bunch-to-bunch spacing (physically quite reasonable). If, on the other hand, we want to be able to observe the beam spectrum up to the single-bunch roll-off frequency, then the pickup must be short with respect to the length of the individual bunches.

a. The single-plate capacitive pickup

When the capacitor plate, or button, in Fig. 10 is exposed to the electric field of the beam, the image charge on the plate will be related to the beam current I_B by

$$q = -g\ell I_B/\beta c \tag{7.1}$$

where q and I_B are phasor quantities, ℓ is the effective electrode length, and the geometric factor g has the same significance as in Green's reciprocation theorem (Sect. 1a) of fractional image charge (per unit length). The latter two quantities are determined by the electrode size and distance from the beam I_B of positive particles; if the electrode completely encircled the beam, the factor g would be unity.

Associated with q is a charging current $I_C = \partial q/\partial t = j\omega q$ which flows through the *series* combination of R and C, causing a voltage across R of

$$V = -j\omega q \frac{R}{1+j\omega RC} = I_B j\, g \frac{\omega \ell}{\beta c} \frac{R}{1+j\omega RC} \tag{7.2}$$

which, from Eq. 4.12, yields a transfer impedance of

$$Z_p = j\, g\, \ell k_B \frac{R}{1+j\omega RC} \tag{7.3}$$

Although with an unmatched load the equations for shunt impedance are not strictly appli-

cable, we can use them to find an effective RT^2 for this pickup case:

$$RT^2 = (g\ell k_s)^2 \frac{4R}{1 + (\omega RC)^2} \tag{7.4}$$

At low frequencies, the signal is proportional to the rate of change of beam current, but above $\omega RC \approx 1$, the capacitance is said to "integrate" the signal and the resulting response is

$$Z_p \rightarrow g\ell/\beta cC \tag{7.5}$$

just the result we would have obtained had we assumed that the voltage across C (and R) was simply qC, i.e. that the charge on the grounded plate of C instantly equilibrated to the image-current charge. Note that for all the above equations, for an arbitrarily shaped electrode of area A at a distance a from the beam, we can approximate the product $g\ell$ by $A/2\pi a$, so that we can rewrite Eq. 7.5, for example, as

$$Z_p \rightarrow \frac{A}{2\pi a\, \beta cC} \tag{7.6}$$

and similarly for Eqs. 7.3 and 7.4. This region of flat response is often used for the observation of beam current versus time with a wide frequency range; however, because it calls for $RC > 1/\omega$, extending the region to lower frequencies usually entails raising C, i.e. reducing the flat-region gain.

Capacitive pickups are used at the LBL Advanced Light Source (ALS) as beam-position monitors. The ALS is a 1.5 GeV, high-current electron synchrotron storage ring, requiring a large number of such monitors, and so, as mentioned earlier, these conditions dictated a small-sized, low-impedance pickup. The electrodes are in the form of roughly 1 cm diameter discs located approximately 2.5 cm from the beam, and having a capacitance of approximately 25 pf. The output is fed directly into a 50 ohm coaxial line (which therefore serves as the load "resistor"), so that the low-frequency roll-off point is roughly 125 MHz, which is low enough to permit observation of the strong coherent line at the fundamental of the rf frequency, 500 MHz. A rough estimate of the transfer impedance using Eq. 7.5 gives .07 ohms, in reasonable agreement with the measured value of 0.1 ohm. The corresponding shunt impedance (based on the latter number) gives 0.8 mΩ, so that even with hundreds of such electrodes in the machine, their total beam impedance of only a fraction of an ohm.

b. The Resonated Capacitive Pickup

By placing an inductor in parallel with C, as in Fig. 11, we not only get a stronger response (albeit over a narrower frequency band), but we obtain, at resonance, a resistive device which can be made to serve as a matched load, and hence used as a kicker. Under these circumstances, the external resistor is no longer an intrinsic part of the circuit (e.g., necessary to provide a charging path for C, and so R in Fig. 11 will be used to represent the total circuit losses due to the combination of the pickup and the inductor. We begin our discussion by considering a long-plate device, in some sense a prologue to the stripline electrode described in the next section, and then consider the limiting case of a resonated button capacitor.

Let us consider the capacitor plate as a center-driven open transmission line of total length ℓ and characteristic impedance Z_L. From standard transmission line theory we find that the open line presents at its center an impedance of $-(j/2)\, Z_L \cot(k_L \ell/2)$ (plus

losses), i.e. for $k_L \ell < \pi$ it behaves like a capacitance. If we denote the unloaded quality factor of the circuit by Q, at the resonant frequency, $Q = R\omega_r C$, so that

$$R = \tfrac{1}{2} Q Z_L \cot (k_L \ell/2) \tag{7.7}$$

where in Eq. 7.7, k_L is now the transmission-line wave number at the resonant frequency.

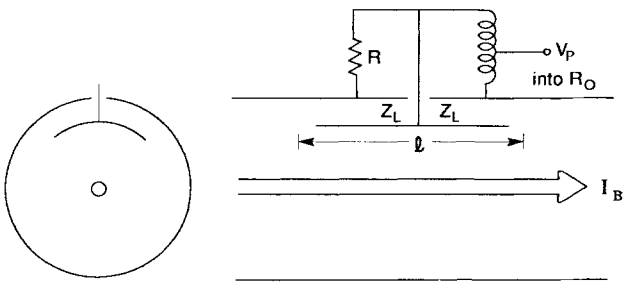

Fig. 11. Resonated Capacitive Plate

If we excite the plate as a kicker with a voltage V_o at the center point, the voltage at the ends of the line (i.e., the plate) will be V_o sec $(k_L \ell/2)$. If we assume that the longitudinal fields at the ends of the plate are concentrated in a distance short compared with $1/k_L$ so that the transit time factor associated with them is negligible, the beam voltage at the outer wall, as defined by Eq. 4.2, can be approximated by

$$V_{wall} = \int_{<-\ell/2}^{>\ell/2} E_s e^{jk_B s}\, ds \cong V_o \sec (k_L \ell/2) \left[-e^{-jk_B \ell/2} + e^{jk_B \ell/2}\right] \tag{7.8}$$

where the inequality signs in the above integrals are merely to indicate that the integration limits are sufficiently beyond the ends of the plate to include the full effect of the end-gap fields. Using the arguments made at the end of Sect. 2, we can now obtain the beam voltage at the location of the beam which, after some rearrangement of terms gives

$$V = g\, V_{wall} = 2j\, g\, V_o \frac{\sin (k_B \ell/2)}{\cos (k_L \ell/2)} \tag{7.9}$$

We can now use Eq. 4.9 to obtain the shunt impedance, by noting that the power to the kicker is simply the power dissipated in R, namely $V_o^2/2R$, whereby

$$R_{\|} T^2 = 2\, Q\, Z_L\, g^2 \frac{\sin^2 (k_B \ell/2)}{\cos (k_L \ell/2) \sin (k_L \ell/2)} \tag{7.10}$$

from which, using Eq. 4.23 with $Z_c = R_O$, we obtain

$$|Z_P| = g \sin(k_B \ell/2) \sqrt{\frac{R_o Z_L Q}{\cos k_L \ell/2 \sin k_L \ell}} \tag{7.11}$$

To find the short-plate or button limit, we apply the usual small angle approximations to Eq. 7.11 and convert the line impedance to the total capacitance using

$$Z_L = \ell / v_L C \tag{7.12}$$

to obtain

$$Z_P = \frac{g\ell}{2\beta c} \sqrt{\frac{\omega_r R_o Q}{C}} \tag{7.13}$$

Comparison with Eq. 7.5 shows that the transfer impedance for the resonated capacitive button is a factor of $Q/2$ greater than the high-frequency limit of the resistively loaded one.

Because the single-plate g-factor is position-dependent, it is customary to use a pair of plates, adding their signals to obtain a longitudinal signal, and differencing them to obtain a transverse one. We will defer a detailed discussion on sum and difference behavior, , as well as the relevant g-factors and methods by which they can be calculated, until the following section on stripline electrodes.

A recent application of tuned-plate detectors for measuring the position of small extracted beam currents at Fermilab [18] has been able to resolve transverse beam position to within 0.1 mm at a beam current of 1.7×10^{-8} ampere using plates one meter long. The circuits operate at 53.1 MHz (the Tevatron rf frequency, and hence a frequency at which there is a strong coherent signal) and have an unloaded Q of about 380.

8. Stripline Electrodes

We have referred earlier to the use of stripline electrodes as pickups/ kickers, and mentioned that in a sense the stripline pair can be thought of as a realization of the parallel-plate pickup in which the electrode structure has a characteristic (real) impedance. We begin this section with a description of the electrode structure and the electromagnetic fields. Following this we will calculate the various response functions; for pedagogical purposes, we will analyze the pickup behavior directly using the image-current approach, as well as obtaining it from the kicker performance using reciprocity.

a. Stripline Geometry and Electromagnetic Fields

A schematic model of a stripline electrode pair is shown in Fig. 12. Each of the stripline plates with its adjacent ground plane (walls) forms a transmission line (for TEM waves) of characteristic impedance Z_L. The output signal line is likewise assumed to be of impedance Z_L; typically the output line impedance will subsequently be transformed to some standard output impedance Z_c. In the center (away from the ends) of these short lines the fields are purely transverse and propagate at a line velocity v_L. That velocity would be the velocity of light for smooth two-dimensional conductors, but may be reduced by the presence of magnetic or dielectric media or by longitudinal variations in the cross sections of the conductors. Excitation of/by the beam takes place at the gaps at the ends of the line, where longitudinal fields occur.

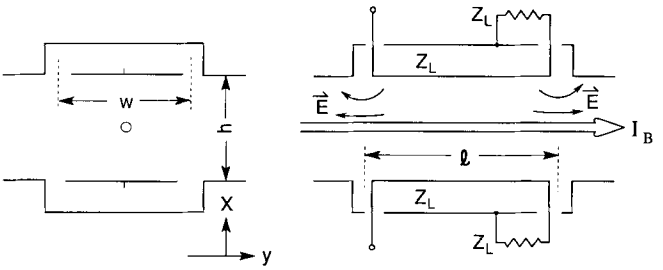

Fig. 12. Schematic representation of a pair of stripline electrodes. The left-hand figure views the structure looking along the beam; the right-hand figure, looking perpendicular to it.

Although concentrated in the region of the plates, the fields of each line extend into the region between them (as of course they must, in order for the electrodes to interact with the beam) where they overlap. The resulting coupling of the two lines produces two characteristic modes of joint excitation, as shown in Fig. 13. In the first of these, the voltages on the upper and lower striplines are of equal magnitude and are in phase; in the second, they are also of equal magnitude but 180° out of phase. The former mode, as we shall see, is associated with the device's use as a longitudinal pickup/kicker; the latter, as a transverse one. Because of the relative phases of the individual signals, these two modes are frequently known as sum and difference modes, respectively. It generally turns out that the two modes have slightly different characteristic impedances, a complication we shall usually ignore in the following discussion.[12] Because in either the sum or difference mode equal signals appear on both striplines, if they are symmetrically driven and/or loaded, we can treat the two striplines as independent transmission lines, each with a characteristic impedance twice that of the combined line, rather than as a single bi-filar line.

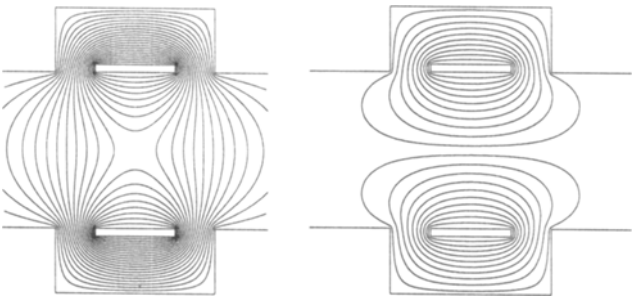

Fig. 13. The sum (left-hand figure) and difference (right-hand figure) modes of a stripline pair. The "field" lines represent equipotentials of the beam voltage, or more accurately, equipotentials of the equivalent two-dimensional electrostatic problem (see text).

[12]The situation is analogous to that of the coupled motion of two identical pendula. That system has two characteristic modes, in the first of which the two pendula oscillate in phase, in the second, 180° out of phase; analogous to the two different stripline impedances, the two pendulum modes have different oscillation frequencies.

b. Pickup Analysis Using Image Currents

Let us depart from our usual practice, and regard the current shown in Fig. 12 as being a short pulse in the *time* domain, $i_B(t)$. We assume that each of the plates intercepts a fraction g of the image current (we neglect for the moment any possible distinction between the g's associated with the two modes of excitation).

When the pulse reaches the upstream end of the stripline, it repels positive charges into the output line and along the stripline. Since both lines are of impedance Z_L, half the image charge goes into each, and a signal of $\frac{1}{2} g i_B(t) Z_L$ propagates both in the output line and downstream (with velocity $\approx c$) on the stripline. At time ℓ/c later the beam, also assumed to move at c, and this latter pulse both arrive at the downstream end, where the departing beam releases a *negative* current pulse of $-g i_B$. As at the upstream end, the pulse divides, with the downstream half cancelling the positive pulse from the upstream end, and the other half propagating *up*stream,[13] where it enters the output line at time $2\ell/c$, and is seen as a negative pulse of voltage $-\frac{1}{2} g i_B(t) Z_L$. Hence the pulse emerging from the output line is a bi-polar pulse whose two lobes as separated by time $2\ell/c$. If one Fourier analyzes the response to an infinitely sharp pulse of unit amplitude, one obtains the the response function for a single stripline

$$Z_P = \frac{g}{2} Z_L (1 - e^{-j\ \omega \ell c}) = g\, Z_L\, e^{j(\pi/2 - k_o \ell)} \sin k_o \ell \tag{8.1}$$

The single-plate g-factor is (transverse-) position sensitive. However, to first order the sum of the g-factors of the upper and lower plates, which we will define as $g_{\|}$, is constant. Hence by summing the output of the two plates, we obtain a relatively position-independent longitudinal signal which is simply proportional to $(1/\sqrt{2})\ g_{\|}$.[14] If we then transform the signal to a "standard" output impedance Z_c (e.g. 50 ohms) we obtain for the longitudinal transfer impedance

$$Z_P = \sqrt{\frac{Z_L Z_c}{2}}\ g_{\|}\ e^{j(\pi/2 - k_o \ell)} \sin k_o \ell \tag{8.2}$$

Because the *difference* in the g-factors of the two plates is to first order proportional to the transverse position of the beam, we can obtain a transverse signal by taking the difference of the signals from the two striplines. To obtain a position-independent transverse g-factor $g_{\perp}$, we would need to divide the difference in the individual g-factors by x; to keep $g_{\perp}$ dimensionless, we divide instead by x/b, where $b = h/2$ is the half-gap. Using the definition of transverse transfer impedance (Eq. 4.13) and again transforming to an output impedance of Z_c ohms, we obtain the result

$$Z_P' = \sqrt{\frac{Z_L Z_c}{2}}\ \frac{g_{\perp}}{b}\ e^{j(\pi/2 - k_o \ell)} \sin k_o \ell \tag{8.3}$$

We will defer discussion of Eqs. 8.2 and 8.3 until the next subsection.

[13]Note that *no signal* appears at the downstream end (this would have been equally true had the downstream end been connected to a matched output cable rather than a terminating resistor). Hence the stripline is sensitive to the direction of the beam, and is frequently referred to as a *directional coupler*.

[14]A certain amount of confusion may arise from the fact that $g_{\|}$ is defined for the combination of the two striplines, yet Z_L is defined for a single line. The logic behind this disparate treatement is that we want a longitudinal g-factor to be position independent (which means defining it for the pair of striplines), whereas for impedance matching, the relevant quantity is the impedance of the individual striplines.

c. Analysis Based on Kicker Behavior

To calculate the kicker constant (see Eq. 4.1), we must evaluate the integral for the beam voltage along the stripline. Recall from our discussion in Sect. 4b that for directional devices, the beam direction when the device is used as a kicker must be opposite that to its direction when the device is used as a kicker.[15] Hence, for a stripline kicker the beam must move in the direction opposite that shown in Fig. 12. If we define the coordinate of the right-hand gap as $s = \ell$, and the left hand as $s = 0$, and define $t(s = 0) = 0$, then the time along the path in the integral for the beam voltage (see Appendix 2) is $t = -s/v$, giving for the beam voltage integral

$$V = \int_{>\ell}^{<0} E_s(s)\, e^{j\omega t}\, ds = \int_{>\ell}^{<0} E_s(s)\, e^{-jk_B s}\, ds \tag{8.4}$$

As previously, we use inequality signs to indicate that the integration limits are sufficiently beyond 0 and ℓ to include the full effect of the end-gap fields.

If the end gaps are short compared with the relevant wavelengths, we can separate the integral in Eq. 8.4 into two pieces, one for each gap, over each of which the factor $e^{-jk_B s}$ is approximately constant. The beam voltage at the outer wall, across the gap at $s = 0$, is just the the stripline voltage at that point, $V_L(0)$, multiplied by the unit phase factor $e^{jk_B 0}$ (times a transit-time factor which, for short gaps we assume to be unity)[16]; for the gap at $s = \ell$ it is just $-V_L(\ell)$ multiplied by the phase factor $e^{-jk_B \ell}$. Since the wave in the stripline is moving from left to right, we have

$$V_L(\ell) = V_L(0)\, e^{-jk_L \ell} \tag{8.5}$$

we have for the integrated beam voltage at the outer wall

$$V(x=b) = V_L(0)\left(1 - e^{-j(k_B + k_L)\ell}\right) = 2V_L\, e^{j(\pi/2 - \theta)} \sin\theta \tag{8.6}$$

where $\theta \equiv (k_L + k_B)/2$.

Based on the arguments made at the close of Sect. 2, the value of the beam voltage at $x = 0$ is just $g(0)\cdot V(x=b)$, where g is the pickup g-factor for a beam at $x = 0$. Using arguments similar to those made for the stripline pickup, we see that if we put equal voltages on both the upper and lower striplines, then to first order the longitudinal voltage will be position-independent, and given by

$$V_{\|} = 2\, g_{\|}\, V_L\, e^{j(\pi/2 - \theta)} \sin\theta \tag{8.7}$$

For the (only slightly) idealized stripline geometry in Fig. 12, the solution near the lateral centerline of the electrodes can be obtained in closed form:

$$g_{\|} = \frac{2}{\pi} \tan^{-1}\left(\sinh\frac{\pi w}{2h}\right), \tag{8.8}$$

[15] At the conclusion of this discussion it may be useful to the reader to convince himself that in the case in which the wave and beam velocities are exactly equal, for a beam moving in the direction shown in Fig. 12, there is *no* net kick to the beam, analogous to the earlier-noted pickup result.

[16] Refer to our earlier discussion at the conclusion of Sect. 2.

an expression whose value exceeds 0.95 for $w/2h > 1$.

In general, g-factors need to be calculated empirically. If we neglect the transit-time factor in the end-gaps, or at least assume it to be independent of lateral position, then the longitudinal mid-point of the stripline plate defines an equipotential of the beam voltage. Hence at the longitudinal mid-plane, the electrical surfaces shown in the left hand figure in Fig. 12 serve as a suitable boundary for solving Eq. 2.9b., the beam voltage equation. As noted in the discussion following that equation, for highly relativistic particles, that equation reduces to Laplace's equation and so we can calculate V using, for example, a numerical electrostatic solver. From our discussion of the Green's reciprocation theorem, we see that $g(x,y)$ for a given electrode is simply the calculated $V(x,y)$ when that electrode is placed at unit potential, $g_{\|}(x,y)$ is $V(x,y)$ when both electrodes are at positive unit potential, and $g_{\perp}(x,y)$ is $V(x,y)/(x/b)$ when the electrodes are at equal and opposite unit potentials. In fact, the equipotentials in the left and right halves of Fig. 13 were obtained by solving the electrostatic field problems with boundary conditions appropriate to calculating $g_{\|}$ and $g_{\perp}$, respectively.

To power a pair of striplines of impedance Z_L at voltage V_L from a single line of some standard input impedance Z_c, using a matched transformer and splitter, requires an input voltage $V_K = V_L \sqrt{2\, Z_c/Z_L}$. Inserting this expression into Eq. 8.7 and using Eq. 4.1 we obtain for the longitudinal stripline kicker constant

$$K_{\|} = \sqrt{\frac{Z_L}{2\, Z_c}}\, 2\, g_{\|}\, e^{j(\pi/2 - \theta)} \sin\theta \tag{8.9}$$

Inserting Eq. 8.9 into Eq. 4.17, we in turn obtain the longitudinal transfer impedance

$$Z_P = \sqrt{\frac{Z_L\, Z_c}{2}}\, g_{\|} e^{j(\pi/2 - \theta)} \sin\theta \tag{8.10}$$

As expected, this is the same as Eq. 8.2, under the assumption made in deriving that equation that both v_L and v_B are c.

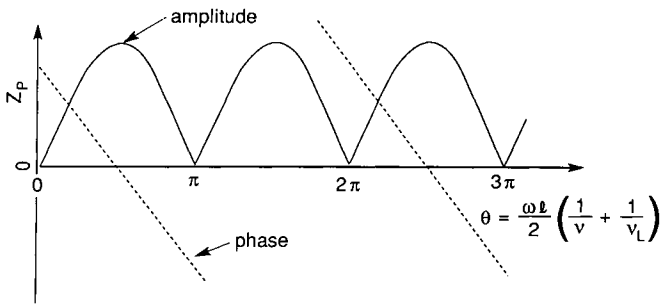

Fig. 14. Amplitude of the longitudinal kicker/pickup response function for striplines.

The amplitude of the kicker/pickup response function is shown in Fig. 14 which may be regarded as the response to either frequency, length, or velocity. If both beam and line velocities equal c, then $K_{\|}$ (or Z_P) is maximum at $\ell = \lambda/4$; for this reason, the electrode is often called the "quarter-wave loop". The reason for the maximum under this condition is quite straightforward. In a pickup, the (sinusoidal) voltage from the downstream gap arrives in phase with that from the upstream gap: There is a delay of $\pi/2$ in generating the downstream signal, an additional $\pi/2$ for it to propagate back to the upstream end, and an additional phase shift of π due to its opposite polarity. Similarly, under this condition, in the kicker the voltage kicks experienced at the upstream and downstream gaps will be in phase (they will be π *out of phase* if the beam passes through in the same direction as in the pickup). From the (square of the) response function it can be seen that the stripline is a broad-band device that provides a bandwidth of one octave width at 1.25 dB down from the maximum, or a 3-to-1 range at 3 dB down.

Power for broad-band, high frequency operation is expensive, motivating one to maximize the shunt impedance which is, using Eq. 4.10

$$R_{\|}T^2 = 2Z_L\, g_{\|}^2 \sin^2\theta \tag{8.11}$$

Note that as mentioned before, in this more fundamental figure of merit the source (or terminal) impedance Z_c does not appear. At frequencies below about 100 MHz, the use of ferrite is very effective for increasing Z_L and shortening the electrode length. On the other hand, because it is necessary to make the electrode width less than $\lambda/4$ in order to avoid parasitic modes, at very high frequencies, a lower ratio w/h may reduce $g_{\|}$; another problem at higher frequencies is that so-called waveguide modes may propagate in the gap h and modify the response.

Typical stripline electrodes [19,20] have single-line impedance in the range 25-to-100 ohms and $g^2 \geq \frac{1}{2}$, giving at maximum response

$$R_{\|}T^2 \approx 25 - 100\ \Omega$$
$$Z_P \approx 18 - 35\ \Omega$$
$$K_{\|} \approx 0.7 - 1.4$$

A recent application of stripline electrodes in which weak signal and costly power were concerns was in the stochastic cooling systems in the Fermilab antiproton accumulator.[21] Stochastic cooling systems require large bandwidth, and, because they require the detection of Schottky signals, also require high-efficiency electrodes. At GHz frequencies, the one-octave bandwidth of striplines meets the former requirement, and as a result of their reduced length (proportional to the wavelength)at these frequencies, the relatively modest shunt impedance could be compensated for by employing large numbers of such loops. (The response of the individual electrodes was itself raised by using a relatively high stripline impedance of $Z_L \approx 100$ ohms.) Electrodes having a response range of 1-to-2 GHz were used in 128-element arrays, giving $R_{\|}T^2 = 128 \times 130 = 16.6\ k\Omega$ and $Z_p = 40\sqrt{128} = 450\ \Omega$.

We now examine the behavior of the same stripline electrode configuration used as a transverse device. As is our wont, we shall calculate the response by applying the Panofsky-Wenzel theorem to the longitudinal fields which are present in the excitation mode for which the device is used as a transverse kicker. Not surprisingly, that again involves exciting the two striplines with voltages of equal magnitude, but with the polarity of the lower being the negative of the upper.

Following the arguments that led from Eq. 8.6 to Eq. 8.7, and invoking the definition of $g_\perp$ (see the discussion preceding Eq. 8.3) we can obtain an equation analogous to Eq. 8.7 for this mode of excitation,

$$V_\perp(x) = 2\, g_\perp \frac{x}{b} V_L\, e^{j(\pi/2-\theta)} \sin\theta \tag{8.12}$$

Note that in this excitation mode, E_s, and hence the beam voltage, are zero for $x = 0$; also, by Green's reciprocity, to the extent that the transverse pickup signal varies linearly with the transverse position, so does the longitudinal kicker voltage in this mode. As with $g_\parallel$, one can obtain a closed-form expression for $g_\perp$; near the centerline, where the linear approximation is accurate, we have

$$g_\perp = \tanh\frac{\pi w}{2h} \ . \tag{8.13}$$

The coupling between the two striplines also changes producing a lower value of Z_L. Following the arguments leading to Eq. 8.9, we obtain for the longitudinal kicker function $K'_\parallel$ for this excitation mode

$$K'_\parallel = \frac{x}{b}\sqrt{\frac{Z_L}{2Z_c}}\, 2g_\perp\, e^{j\left(\frac{\pi}{2}-\theta\right)} \sin\theta \ . \tag{8.14}$$

Applying Eq. 4.7, we obtain for $K_\perp$

$$K_\perp = \sqrt{\frac{Z_L}{2Z_c}}\, 2g_\perp \frac{v}{h\omega} e^{-j\theta} \sin\theta \tag{8.15}$$

This result is very similar to the longitudinal K in Eq. 8.9, but the factor $1/h\omega$ further penalizes (i.e., over and above its adverse effect on g) large aperture, and shifts the frequency for maximum response downward to $\omega = 0$, confirming our earlier observation that, unlike the longitudinal case, a transverse kicker *can* have a dc response.

In fact the transverse kicker response is much like a typical $\sin\theta/\theta$ transit-time response. This will be more recognizable if we rearrange Eq. 8.15 using the definition of θ given following Eq. 8.6

$$K_\perp = \sqrt{\frac{Z_L}{2Z_c}}\, 2g_\perp \frac{\ell}{h}\left(1+\frac{v}{v_L}\right) e^{-j\theta} \frac{\sin\theta}{\theta} \ . \tag{8.15a}$$

Applying Eq. 4.19 to Eq. 8.15, we obtain the transverse transfer impedance

$$Z'_p = \sqrt{\frac{Z_c Z_L}{2}}\, g_\perp \frac{2}{h} e^{j\left(\frac{\pi}{2}-\theta\right)} \sin\theta \tag{8.16}$$

Note that transverse transfer function does *not* contain the $1/\omega$ factor and, except for the small difference between $g_\parallel$ and $g_\perp$ (and numerically different Z_L) is the same as the longitudinal case divided by the half-gap, so that, unlike the longitudinal case, the transverse kicker and pickup exhibit different frequency responses.

The transverse shunt impedance is obtained by applying Eq. 4.11 to Eq. 8.15

$$R_\perp T^2 = 2Z_L\left(g_\perp \frac{2}{k_B h}\right)^2 \sin^2\theta \tag{8.17}$$

As expected, like its longitudinal counterpart, $R_\perp T^2$ is independent of Z_c. The frequency dependence of $R_\perp T^2$ mirrors that of $K_\perp$; it is interesting to note how the $k_B{}^2$ in the numerator of Eq. 4.24 removes that frequency dependence from the transverse pickup output power.

Finally, as we noted earlier, an interesting feature of the stripline pickup is that, if the beam velocity v equals the line velocity v_L, no voltage appears at the downstream end. In principle, this allows that end to be electrically connected to any impedance, including a short or an open circuit, with no effect on the picked-up signal. However, the output line will then not be back-terminated to absorb reflections in the circuit, so in practice this apparently spurious resistor is generally present. (In the case of the stripline *kicker*, the far end of the line [in this case, the *up*stream end] *must* be terminated in a matched load to avoid reflection of the usually sizable kicker signals.)

d. Stripline Beam Impedance

Because it gives a result different from the resistive-wall case, it is of pedagogical interest to look at the beam impedance of the stripline electrode. We will restrict ourselves to the case of the longitudinal impedance at the frequency of maximum response, i.e. the quarter-wave condition; we will leave it as the proverbial "exercise for the reader" to work out the result for the full band, as well as for the transverse case.

Referring to our earlier image-current analysis, and denoting the upper and lower plates with subscripts 1 and 2, respectively, we see that when beam passes the upstream gap, it induces a voltage $g_1 I_B Z_L/2\ (\cdot T)$ in the upper stripline which propagates both downstream and out the signal line. The beam induces an equal and opposite signal (plus a $\pi/2$ phase delay) at the downstream gap, which, when it arrives at the upstream gap is in phase with the upstream-gap signal, thereby doubling it. The beam voltage at the beam location for the upstream gap, which will bring in another factor of gT, is therefore

$$V_1^{up} = -g_1{}^2 I_B\ Z_L T^2 \tag{8.18}$$

On the other hand, when the upstream signal reaches the downstream gap, its phase is such that it will exactly cancel the gap voltage induced by the beam at that point, so there is *no* beam voltage kick at that gap.

In like manner, the total beam voltage due to the signals induced in the lower stripline is $-g_1{}^2 I_B Z_L T$, giving a total beam voltage for the two lines of

$$V = -(g_1{}^2 + g_2{}^2) I_B\, Z_L T^2 \tag{8.19}$$

Dividing by the beam current, and noting that $g_\parallel{}^2 = (g_1 + g_2)^2 \approx 2\,(g_1{}^2 + g_2{}^2)$, we obtain for the longitudinal beam impedance

$$Z_\parallel = g_\parallel{}^2\, Z_L T^2/2 \tag{8.20}$$

Comparison with the maximum shunt impedance given by Eq. 8.11 shows that

$$Z_{\parallel} = R_{\parallel} T^2/4 \tag{8.21}$$

i.e. it is one-*fourth* the longitudinal shunt impedance, rather than one half it, as was the case for the resistive wall or resonant cavity. (It is not meaningful to compare the results for the unloaded devices, where the resistive-wall beam impedance is the same as the shunt impedance, because without a terminating load on the stripline, there would be reflected waves from the upstream end, invalidating the above analysis. In fact it is just this absence of any dissipative load within the stripline which is responsible for the difference in the two results.)

9. Standing-Wave Devices; A Summary

All the devices considered thus far can be categorized as standing-wave electrodes because (regarding them for the moment as kickers) the electromagnetic fields they generate remain localized in space, rather than propagating along with the beam.[17] We can compare expressions for the peak shunt impedances of a variety of standing wave devices (some of these expressions are derived in this note; for others, see Ref. 22). If we introduce the 3-dB bandwidth $\Delta\omega$ (for resonant devices, this means replacing the Q in the formulas by $\omega/\Delta\omega$), and use ℓ for the overall length, we get the relations shown in Table II.

TABLE II

	Longitudinal	Transverse
Stripline Pair		
Non-Resonant; length $\ell = \lambda/4$	$R_{\parallel} T^2 \frac{\Delta\omega}{\omega} = 8 Z_{\parallel} g_{\parallel}^2 \frac{\ell}{\lambda}$	$R_{\perp} T^2 \frac{\Delta\omega}{\omega} = 8 Z_{\perp} g_{\perp}^2 \frac{\ell}{\lambda} \left(\frac{\lambda_B}{b}\right)^2$
Resonant; length $\ell = \lambda/4$	$R_{\parallel} T^2 \frac{\Delta\omega}{\omega} = \frac{32}{\pi} Z_{\parallel} g_{\parallel}^2 \frac{\ell}{\lambda}$	$R_{\perp} T^2 \frac{\Delta\omega}{\omega} = \frac{32}{\pi} Z_{\perp} g_{\perp}^2 \frac{\ell}{\lambda} \left(\frac{\lambda_B}{b}\right)^2$
Inductively resonated; length $\ell \ll \lambda/4$	$R_{\parallel} T^2 \frac{\Delta\omega}{\omega} = 4\pi Z_{\parallel} g_{\parallel}^2 \frac{\ell}{\lambda}$	$R_{\perp} T^2 \frac{\Delta\omega}{\omega} = 4\pi Z_{\perp} g_{\perp}^2 \frac{\ell}{\lambda} \left(\frac{\lambda_B}{b}\right)^2$
Square Cavity	$R_{\parallel}^{110} T^2 \frac{\Delta\omega}{\omega} = \frac{4}{\pi} Z_o T^2 \frac{\ell}{\lambda}$	$R_{\perp}^{210} T^2 \frac{\Delta\omega}{\omega} = \frac{32}{25\pi} Z_o T^2 \frac{\ell}{\lambda}$

The similarities of the functional forms of these gain-bandwidth values can be expected from general considerations of energy storage and flow, (we will discuss these in more detail in Sect. 10); what is notable is that this variety of practical devices shows only a small range in the value of α (typically ~250-1000 Ω) as defined by Eq. 9.1. (For the transverse shunt impedances, there is an additional factor of $[\lambda_B/b]^2$.)

[17] The stripline is in some sense a mixed case. However, because its fields travel in a direction *opposite* that of the beam, it is usually regarded as an SW device. This should be clarified by the discussion in Sect. 10

$$\frac{R_{\|}\, T^2\, (\Delta\omega/\omega)}{\ell/\lambda} = \alpha \tag{9.1}$$

Note that in Eq. 9.1 we consider the product of shunt impedance and *fractional* bandwidth, per unit *fractional* length (of wavelength). To understand better the "normalization" of the bandwidth to the frequency and the length to the wavelength, consider the stripline. It has a roughly 1.5 octave bandwidth irrespective of frequency, and is always (at midband) 1/4 wave long. If we put Eq. 9.1 into the alternate form

$$\frac{R_{\|}\, T^2\, \Delta\omega}{\ell} = \alpha'\, \omega^2 \tag{9.2}$$

we see that, on the one hand, the gain-bandwidth product per unit length increases as the square of the frequency; again thinking of the stripline, this arises because the absolute bandwidth of the octave increases with frequency, as does the number of quarter wavelengths per absolute length. On the other hand, Eq. 9.2 says that, at a given frequency, the overall factor is pretty much the same for all the devices shown. The reader may recall that we mentioned at the beginning of this portion of the report that choice of detector necessitated a trade-off among these quantities; Eqs. 9.1 and 9.2 dramatically illustrate the point. There is one possible exception to the rule, which has thus far had limited practical use with accelerator beams, and that is the subject of the following section.

10. Traveling-Wave Devices

Let us imagine the following two scenarios: Assume that we have a total length ℓ which is occupied by, in one case, a (properly phased) array of standing-wave (SW) kickers, and in the other, by a device capable of generating a voltage wave which moves in the same direction and with the same velocity as the beam; it is standard parlance to refer to this latter as a traveling-wave (TW) device. Let us further assume that the longitudinal fields in both kickers are comparable or, more simply, that they produce the same voltage gain per unit length,[18] V', and that both the *individual* SW devices and the TW device each require the same input power, P_i. For both devices, the total energy gain in length ℓ will simply be $V'\,\ell$. However, the TW device will require an input power of only P_i, whereas, assuming n SW devices are required to span the length ℓ, the array will require an input power of nP_i.

From the definition of shunt impedance (Eq. 4.9), we see that for the TW pickup, RT^2 will be proportional to ℓ^2; in contrast, for the SW array, it will be proportional to ℓ^2/n, or since $n \propto \ell$, simply to ℓ, consistent with the results from Eqs. 9.1 and 9.2. (As implied by the former equation, the SW device actually scales as ℓ/λ, rather than ℓ; the reason for this is that, as a result of transit-time effects, the length of a SW device is perforce limited to being only a fraction of a wavelength).

A similar argument can be made for the efficacy of TW pickups. As we pointed out in the introduction to Sect. 5 (beam impedance), the output power from a pickup comes from the work the beam does against the fields which it itself generates. If we have an array of such pickups, the power will simply be proportional to the overall length, since as the beam moves from pickup to pickup, it must regenerate that self field in each element of the array. If, on the other hand, the self field were to propagate along with the beam, the self-field

[18] i.e., we neglect the packing-fraction problem associated with the arrays

would increase (more or less linearly) as the beam moved constantly added energy to it as it moved along the device (not possible with a standing wave device where, by definition, the field remains in one place), then the self-field would be proportional to the length, and hence the signal power, to the square of the length.

A principal practical problem with TW devices is the difficulty in matching the field wave's (phase) velocity to that of the beam. Because of dispersion, it is not possible to match these velocities exactly over any frequency band; the effect on the bandwidth of the resulting (frequency-dependent) phase slip between wave and beam is what usually limits the length of such devices. Because the phase-slip factor is dependent on the transit time through the device, it is frequently referred to as a transit-time factor (it usually exhibits the familiar sin θ/θ form associated with SW devices) even though its physical origins are somewhat different (the θ for TW devices depends on the *difference* between two wavelengths, whereas for the SW device it depends on only a single one).

An additional difficulty with TW devices is the problem of coupling to them the input and output power. On the other hand, an additional attraction of TW structures (relative to SW ones) is their lesser complexity as rf structures, particularly at frequencies in the multigigahertz range.

We begin our discussion of TW devices by describing three such devices, and presenting their relevant figures of merit. Following this we present a gain-bandwidth scaling law for TW devices somewhat analogous to Eq. 9.2 for SW ones.

a. The Helical Line

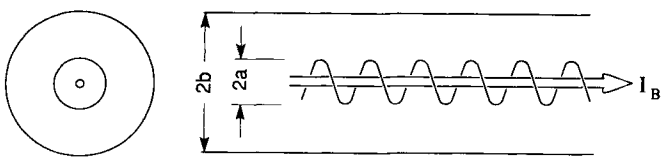

Fig. 15. Beam on the axis of a helical line

A helical line (Fig. 15) is a device in which a wave travelling at c on the periphery of a helix produces an on-axis longitudinal field travelling at reduced velocity $\beta_L c$.[23,24] The shunt impedance of this electrode treated as a sheath helix is shown in Ref. 23 to be given by

$$R_{\parallel}T^2 = \frac{Z_o}{2\pi\beta_L}\left(\frac{h}{\gamma_L}\right)^2\left[\frac{K_o(ha)}{I_o(ha)} - \frac{K_o(hb)}{I_o(hb)}\right]\left(\frac{\sin\theta}{\theta}\right)^2 \qquad (10.1)$$

in which $\gamma_L^2 = 1/(1 - \beta_L^2)$, $h = k_o/\beta_L\gamma_L$, and $\theta = (k_B - k_L)\ell/2$. The modified Bessel functions I_o and K_o for small arguments, that is, for $\beta_L\gamma_L\lambda_o > b$ reduce to the form

$$R_{\parallel}T^2 \approx \frac{Z_o}{2\pi\beta_L} \ln\frac{b}{a}\left(\frac{k_L \ell}{\gamma_L^2}\frac{\sin\theta}{\theta}\right)^2 \tag{10.2}$$

In this we recognize $(Z_o/2\pi)\ln(b/a)$ as the impedance of a coaxial line of radii a and b. Also, we see $\sin\theta/\theta$ as the transit-time factor in which θ is a measure of the phase slip between beam and traveling wave. To avoid large dispersion in the wave velocity in this periodic structure, $\beta_L\lambda_\rho$ (the wavelength of the slow on-axis wave) must be greater than twice the pitch of the helix. In an example use, [25] the helix was effective at $f = 200$ MHz and $\beta = 0.5$. However, the factor γ_L^{-4} makes the device ineffective for very relativistic particles.

b. The Slotted-Coax Coupler

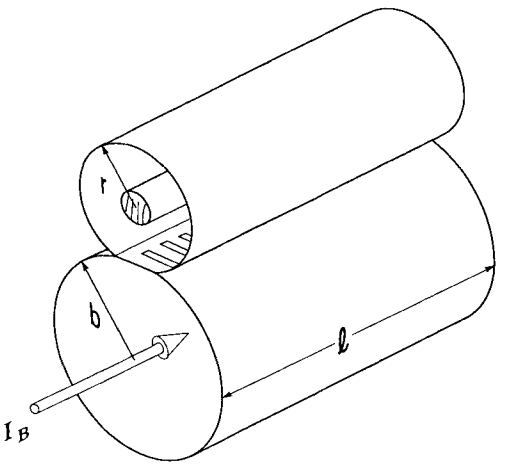

Fig. 16. Slotted-coax coupler attached to a beam tube

The slotted-coax coupler shown in Fig. 16 communicates with the beam tube through a row of holes or slots in the outer wall of a coaxial line parallel to the beam. There is a net energy transfer from a beam particle to the coaxial line until either an equilibrium is reached (there is an equal energy flow back from the coax wave to the beam), or a sufficient phase difference develops between beam and coax signal (the slots that provide the coupling also reduce the phase velocity in the coax and cause dispersion in that velocity). Perturbation calculations [26] for the geometry of Fig. 16 show that the coupling and the velocity are so related that the pickup impedance becomes simply

$$Z_p = -j\frac{k_o \ell\, r}{2\gamma_L^2 b}\sqrt{Z_L R_o}\, e^{-j\theta}\frac{\sin\theta}{\theta} \tag{10.3}$$

where Z_L is the impedance of the coax and γ_L and θ are as in Eq. 10.1. The shunt impedance is then

$$R_{\|}T^2 = Z_L \left(\frac{k_o \ell r}{\gamma_L^2 b} \frac{\sin\theta}{\theta} \right)^2 \tag{10.4}$$

This is very similar to the result for the helix, but here a very small velocity reduction introduces dispersion that limits the use of the slotted coupler as a broad-band device to $\beta_L >$ ~ 0.95. Although it is a weak coupler, it is a good high-frequency structure and is useful where strong coupling is not demanded. In this role it has been used in cooling the antiproton stack in the CERN AA ring. [26]

c. The Wall-loaded TM Waveguide

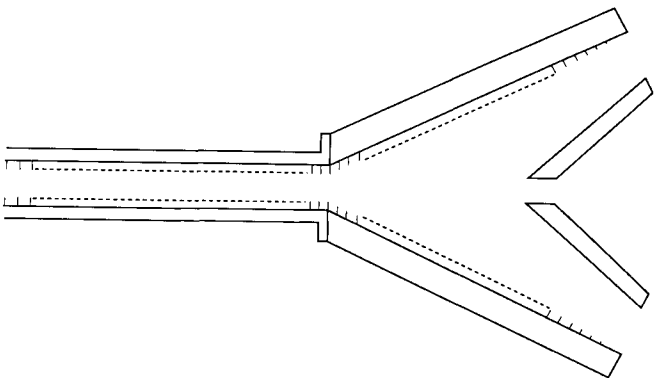

Fig. 17. Downstream end of a corrugated-wall-waveguide pickup

The phase velocity of a TM waveguide can be reduced to correspond to beam velocity by loading its walls with a dielectric liner or with corrugations. Linacs employ such structures. A corrugated guide has been developed [27] for experiments on stochastic cooling in the CERN SPS. This difference pickup is sketched in Fig. 17. It has a bandwidth of about 1 GHz at an operating frequency of 11 GHz. The aperture is 16 x 22.9 mm and the length of the guide is 0.3 meter. Its relevant figures of merit are

$$R_{\perp}T^2 = 1.76 \times 10^4 \text{ ohm}$$

and

$$Z'_P = 108 \text{ ohm/mm.}$$

If we compare the product of shunt impedance and bandwidth per unit length for the TW device with what could be realized with a SW device such as a stripline [21], we find that the former outperforms the latter by roughly a factor of 2.5, and has the additional virtue of being able to operate at high frequency without the penalty for large aperture that the $(\lambda_B/b)^2$ term imposes on transverse SW devices. Designing such a loaded guide is rather straightforward; the major development effort has gone into the transition from the waveguide to the output coaxial signal line.

d. The Gain-Bandwidth Product for TW Devices

We can inquire if the TW structure, like the SW (see Eqs. 9.1 and 9.2), has a gain-bandwidth product proportional to length. But for reference, let us first consider the origin of that factor for a typical SW device, say a cavity with bandwidth $\Delta\omega = \omega/Q$. Its kicker power is given by Eq. 6.1 as

$$P = \frac{V^2}{2R\,T^2} = \frac{\omega U}{Q} \tag{10.5}$$

where U is the field energy contained within the device's volume. From these relations, we find

$$R_{\|}T^2\,\Delta\omega = \frac{V^2}{2U} \tag{10.6}$$

which is proportional to length (U is proportional to length, and as we have already discussed, V^2 is proportional to length-squared).

To obtain an equivalent starting point for the TW structure, if the field propagates within the device at group velocity v_g, exiting at the downstream end into a matched load, then the input power is just the energy per unit length times the group velocity

$$P = \frac{v_g\,U}{\ell} \tag{10.7}$$

$$R_{\|}T^2 = \frac{V^2\,\ell}{2v_g\,U} \tag{10.8}$$

which, as expected, is proportional to ℓ^2. We shall then define the bandwidth by obtaining the frequencies $\pm\,\Delta\omega/2$ at which the transit time factor drops to $1/\sqrt{2}$. T is given by

$$T = \frac{1}{\ell}\int_{-\ell/2}^{\ell/2} e^{jk_B s}\,e^{-jk_L s}\,ds = \frac{\sin\theta}{\theta} \tag{10.9}$$

where $\theta = (k_L - k_B)\,\ell/2$. At $\pm\,\Delta\omega/2$, θ has the value $\theta = \theta_1 = \pm\,1.39$ radian. If we assume θ varies linearly with ω, then to first order we have

$$\theta_1 \approx \frac{\Delta\omega}{2}\frac{d\theta}{d\omega} = \frac{\Delta\omega\,\ell}{4}\left(\frac{dk_L}{d\omega} - \frac{dk_B}{d\omega}\right) \tag{10.10}$$

Using $k = \omega/v_B$ and $dk_L/d\omega = 1/v_g$, we find

$$\Delta\omega \approx \frac{4\theta_1}{\ell}\left(\frac{1}{v_g} - \frac{1}{v_B}\right)^{-1} \tag{10.11}$$

Combining this with Eq. 10.8 and the value of θ_1, we get

$$R_{\|}T^2\,\Delta\omega \approx \frac{V^2}{U}\,\frac{2.8}{1-v_g/v_B} \tag{10.12}$$

Hence we see that, due to transit time effects, the product of gain-per-unit-length and bandwidth is proportional only to length, as is the case for SW devices; however, comparison with Eq. 10.6 also shows that because the denominator in Eq. 10.12 can (in principle, at least) be made quite small, the TW structure can reasonably be a much stronger pickup than the standing-wave type. This last relation stands as a guide for the further development of TW devices as beam detectors.

Acknowledgements

We would like to thank Ms. Diana Morris and Olivia Wong for their invaluable assistance in the preparation of the manuscript, and to Mel Month for his patience and encouragement in seeing the work through to its completion.

This work was supported by the Director, Office of Energy Research, Office of High Energy and Nuclear Physics, High Energy Physics Division, of the U.S. Department of Energy under Contract No., DE-AC03-76SF00098.

APPENDIX 1: REVIEW OF RELATIVISTIC DYNAMICS

One difficulty in writing for a broad audience is the variety of backgrounds of the readers. Instrumentation engineers may find some of the following material helpful in understanding some of the derivations and approximations given in the text; on the other hand, re-cycled particle physicists may find much of it trivial.

The two important dynamical quantities we will be dealing with are the momentum and the energy, whose relativistic definitions are

$$\mathbf{p} = m\,\gamma\,\mathbf{v} \tag{A.1.1}$$

$$E = m\gamma c^2 \tag{A.1.2}$$

where

$$\gamma \equiv \sqrt{1 - v^2/c^2} \tag{A.1.3}$$

In the non-relativistic limit where $v << c$, $\gamma \rightarrow 1 + v^2/2c^2$, and so $\mathbf{p}$ reduces to the classically familiar $m\mathbf{v}$, and E becomes $mc^2 + 1/2\ mv^2$, the familiar classical kinetic energy term, augmented by the now famous Einstein mass-energy term.

In virtually all the situations we will be dealing with, the transverse (x,y) velocities will be negligible with respect to the longitudinal velocity. Several consequences follow from this. The quantity γ will depend only on the longitudinal velocity, i.e. it will be unaffected by changes in the transverse momentum. The direction $\mathbf{s}$, defined by the particle's motion, will be regarded as identical to the z direction, defined by the longitudinal axis of the beamline hardware (which, incidentally, also defines the transverse directions). It is customary in relativistic parlance to define β as the ratio v/c; for highly relativistic particles $\beta \approx 1$, implying that changes in energy and longitudinal momentum are reflected primarily in changes in γ, rather than in particle speed. Consequently, it will

be assumed that in the course of traversing a kicker, along the straight line which the particle moves, s and t are related by $v = \beta c = ds/dt$ and v is assumed to be constant; we will refer to this assumption of straight-line trajectory at constant speed as the *constant velocity approximation.* We should probably note explicitly that the approximation of local horizontal straight-line motion within a kicker is not inconsistent with a deflection on the order of a centimeter some tens of meters downstream, as a result of the *relatively* small transverse momentum imparted by the kicker.

In common parlance, Newton's second law is expressed as $\mathbf{F} = m\mathbf{a}$. A non-relativistically equivalent form, which unlike the above one, generalizes correctly to the relativistic case when the relativistic form of $\mathbf{p}$ (Eq. A.1.1) is used, is

$$\mathbf{F} = d\mathbf{p}/dt \tag{A.1.4}$$

whereby we see that the total kick imparted by a force $\mathbf{F}$ acting along the path traversed by a particle as it moves from point a to point b is given by

$$\Delta\mathbf{p} = \int_{t_a}^{t_b} \mathbf{F}(\mathbf{s}(t),t)\, dt \tag{A.1.5}$$

where we have explicitly allowed for the variation of the force with position as well as time, showing that in that case it will also be necessary to know the position as a function of time. If we now invoke the constant-velocity assumption, we can convert s to a scalar variable and substitute $dt = ds/\beta c$, enabling us to rewrite the integral in the form

$$\Delta\mathbf{p}\beta c = \int_a^b \mathbf{F}(s)\, ds \tag{A.1.6}$$

For the longitudinal component of the momentum, Eq. A.1.6 gives

$$\Delta p_{\|}\beta c = \int_a^b F_s(s)\, ds \tag{A.1.7}$$

If we now consider the energy change over the same path, it is given by

$$\Delta E = \int_a^b \mathbf{F}\cdot\mathbf{ds} = \int_a^b F_s\, ds \tag{A.1.8}$$

Comparison of Eqs. (A.1.7) and (A.1.8) shows that

$$\Delta E = \beta c\, \Delta p_{\|} \tag{A.1.9}$$

It is left as an exercise for the reader to show that the same result could have been obtained by using Eq. A.1.3 to show that

$$d(\beta\gamma) = (\beta + \gamma\frac{d\beta}{d\gamma})\, d\gamma = \frac{d\gamma}{\beta} \tag{A.1.10}$$

and calculating the differentials of energy and momentum directly from Eqs. A.1.1 and 2.

For longitudinal motion, the two quantities ΔE and $\beta c\Delta p$ turn out to be physically equivalent. Because the former form is more intuitive, and because of its ready identification with the beam voltage, we use it to define the performance of longitudinal kickers. The two quantities are *not* physically equivalent for transverse motion, and it proves to be only the latter form which is physically meaningful for transverse devices. (For highly relativistic particles $\beta \approx 1$, and so some authors, particularly those writing on *beam* impedance, define the transverse beam voltage as $c\Delta p_\perp$. The only effect of this is to redefine slightly some of the figures of merit for pickup and kicker performance [see Sect. 4]; the actual values of physical quantities calculated using these re-defined quantities, such as transverse momentum changes, will be unaffected by such change in definition.)

APPENDIX 2: INTEGRALS INVOLVING TIME-VARYING FIELDS

1. Defining the Variables

Consider the integral given in Eq. 1.5, reproduced below, which describes the momentum change imparted to a particle by a kicker. Integrals such as this, as well as their time derivatives, appear throughout the text. The form in which the equation appears is actually a shorthand version; not only does it not show that that the position and time coordinates along the integration path are interrelated, it does not even show the explicit dependence of the fields on those coordinates.

$$\Delta \mathbf{p} = e \int_{t_a}^{t_b} (\mathbf{E} + \mathbf{v} \times \mathbf{B})\, dt \tag{A.2.1}$$

Because fully expanded versions of equations such as this are cumbersome to write out, we will generally employ the above shorthand form. A principal purpose of this appendix is to show the reader how to translate from the shorthand to the fully expanded form so that he can use the equations in this lecture to do his own calculations.

Taking into account that each of the fields in Eq. A.2.1 depends *separately* on space and time, and recalling our earlier assumption that the particle moves along a trajectory of constant x,y, we can rewrite the equation in the more general form

$$\Delta F = \int_{t_a}^{t_b} f(s,t)\, dt \tag{A.2.2}$$

Despite the separate dependence of f on s and t, the s and t appearing in the integrand are related by the trajectory of the particle. In particular, if we assume the uniform, straight-line trajectory described in Appendix 1, and assume that the entrance and exit points a and b are separated by a distance ℓ, we have for the points along the path

$$s = a + v(t - t_a) \qquad t = t_a + (s - a)/v \qquad \text{(A.2.3.a,b)}$$

whereby

$$\frac{ds}{dt} = v = -\frac{ds}{dt_a} \qquad \text{(A.2.4)}$$

and

$$t_b = t_a + \ell/v \qquad \text{(A.2.5)}$$

Hence we can write Eq. A.2.2. in the form

$$\Delta F = \int_{t_a}^{t_b = t_a + \ell/v} f[s(t,t_a),t]\, dt \qquad \text{(A.2.6a)}$$

where we have used $s(t.t_a)$ to indicate the time dependence of s given by Eq. A.2.3.a. Because of the relation between s and t, we could just as easily have expressed the integrand, *as well as the integration limits,* as functions of s, in which case Eq. A.2.2 would have taken the form

$$\Delta F = \int_{a}^{b=a+\ell} f[s,t\,(s,t_a)]\, ds \qquad \text{(A.2.6b)}$$

2. Time-dependence of the Integrated Quantities

From a casual examination of an equation such as Eq. (A.2.1), it might appear that the time dependence of $\Delta\mathbf{p}$ has been "integrated away." Yet from simple physical considerations, we see that this conclusion is manifestly incorrect: A kicker with time-varying fields will impart a momentum change which varies with time.

The answer to the apparent paradox can be seen by examining the more explicit expressions given by Eqs. A.2.6a,b; in those equations, t, the time along the path, merely serves as the parameter characterizing the infinitesimal kick $d\mathbf{p}$ which the particle receives at each point; integrating over t is simply adding up the kicks. The time variable on which the total momentum change depends is a "real-world" time, e.g., the actual time at which the particle enters (or, equivalently, emerges from) the kicker, i.e., t_a. Hence the time variation of those quantities is obtained by differentiating with respect to, in this case, t_a.

When obtaining the time dependence, it is generally easier to convert the integral to the form A.2.6b, where t_a appears only in the integrand, and not in the limits as well. (In the case of the $\mathbf{v} \times \mathbf{B}$ integrand, this conversion occurs naturally since $\mathbf{v} \times \mathbf{B}\, dt = d\mathbf{s} \times \mathbf{B}$.) In that case the time derivative takes the form

$$\frac{d}{dt_a}\Delta F = \frac{1}{v}\int_{a}^{b=a+\ell} \frac{\partial}{\partial t} f[s,t\,(s,t_a)]\, \frac{dt}{dt_a}\, ds = \frac{1}{v}\int_{a}^{b=a+\ell} \frac{\partial}{\partial t} f[s,t\,(s,t_a)]\, ds \qquad \text{(A.2.7)}$$

It is an instructive exercise–one we leave to the reader–to demonstrate that the same result is obtained when one differentiates the expression for ΔF in the form it appears in Eq. A.2.6a (where one must differentiate the limits as well). In fact, the reason we have included the apparently trivial intermediate step in Eq. A.2.7 is to remind the reader that when differentiating under the integral sign in Eq. A.2.6a, t_a appears in the s term, and so the partial derivative must be with respect to s.

We should also mention an important *caveat* when applying Eq. A.2.7 to electromagnetic fields. When using the Maxwell Equations to relate partial space- and time-derivatives, one must *not* take into account the trajectory relation between s and t when taking the derivatives; rather one treats them as independent variables when differentiating, and only afterwards relates them in order to carry out the integration.

Finally, note the following bit of sleight of hand. If we convert Eq. A.2.7 back to an integration over time, we can write it in the form

$$\frac{d}{dt_a}\Delta F = \int_{t_a}^{t_b = t_a + \Delta t} \frac{\partial}{\partial t} f[s,t]\, dt \qquad \text{(A.2.8)}$$

making it appear that we simply got the result by (illegally) differentiating Eq. A.2.6a under the integral sign with respect to the integration variable. In fact, that is *not* what Eq. A.2.8 implies. In Eq. 2.6a, s is a function of both t.and t_a, whereas the form of the integrand in Eq. 2.8 is intended to imply that differentiation takes place with respect to only the *explicitly* time-dependent part of f, and that the substitution of $s = s(t.t_a)$ takes place only *after* differentiation. In fact the outcome of Eq. A.2.8 is somewhat fortuitous (note that the derivative on the left hand side is with respect to t_a, not t), and results from the independence of ds/dt on t_a, a consequence of the constant-velocity approximation.

3. Integrals Involving Phasors

In the course of these notes, we encounter a number of integrals involving phasor quantities, i.e. quantities whose time-dependence takes the particularly simple form $e^{j\omega t}$., to which we can specialize the results of the preceding sections. In many of these integrals there appears, at some point, the related factor e^{jks}. We will see that, despite the similarity of appearances, this latter factor may arise from different causes, and therefore have different physical significance.

a. Total Energy Gain, and Related Integrals

The energy gain for a particle in a kicker is generally written in the form

$$V = \int_a^b \mathbf{E} \cdot \mathbf{ds} \qquad \text{(A.2.9)}$$

where $\mathbf{E}$ is a phasor of the form $\mathbf{E}(x,y,z)\, e^{j\omega t}$. Under the constant-velocity assumption and using Eq. A.2.3b, we can write Eq. A.2.9 in terms of distance alone

$$V = \int_a^b \mathbf{E}(x,y,z) \cdot \mathbf{ds}\ e^{j\omega t} = e^{j\omega(t_a - a/v)} \int_a^b E_s\, e^{jk_B s}\, ds \qquad \text{(A.2.10)}$$

where k_B is the *beam* wave number $k_B = \omega/v$.

Note that the "spatial" exponential factor $e^{jk_B s}$ has *nothing* to do with the (instantaneous) spatial dependence of either **E** or of the beam. In fact, **E** *may* have a spatial, i.e., an s-dependence: In the event that it has none or is a purely real function of s, the **E** field will simply be a standing wave. On the other hand, for, e.g., a travelling wave kicker, the **E** field will have its own $e^{\pm jk_F s}$ dependence (the respective signs depending on whether the field is propagating upstream or downstream); in this case $k_F = \omega/v_F$ is the *field* wave number, where v_F is the wave velocity of the field (usually different from c).

Note also that either by applying Eq. A.2.8 to the first integral, or differentiating the second with respect to t_a we get for the time derivative

$$\frac{\partial V}{\partial t_a} = j\omega \int_a^b \mathbf{E}(x,y,z) \cdot \mathbf{ds}\ e^{j\omega t} = j\omega\ e^{j\omega(t_a - a/v)} \int_a^b E_s e^{jk_B s} ds \qquad \text{(A.2.11)}$$

In addition to the $e^{j\omega(t_o - v/s)}$ term, an additional phase factor may emerge as a result of the integration. In bunched-beam machines, the overall phase of the kicker is generally adjusted so that the field maximum coincides with the arrival time of the beam bunch; hence we will in general implicitly set this phase factor equal to unity, i.e., for purposes other than calculating the time derivative, we will generally ignore it. The following section may help clarify this point.

b. Transit-Time Factor

It is informative to compare the integral in Eq. A.2.10 with that which would result from calculating the instantaneous "voltage" (i.e., integrating at constant t)

$$V_o = e^{j\omega t} \int_a^b E_s ds \qquad \text{(A.2.12)}$$

appearing across the kicker. The ratio of the magnitudes of these two quantities is defined as T, the so-called transit-time factor.

$$|V/V_o| \equiv T \qquad \text{(A.2.13)}$$

As the name implies, T simply represents the reduction in energy gain due to the fact that, because of the finite transit time of the beam through the kicker, it may not experience the (time-) maximum field everywhere along its path. The following example serves to illustrate this point.

Longitudinal kickers with a voltage gap are excited in a mode in which the longitudinal field is essentially constant, i.e. $E_s(s) = E_o$. If the accelerating gap in such a kicker is of length ℓ, we see from Eq. A.2.10 that the voltage gain of such a particle is given by

$$V = e^{j\omega(t_a - a/v)} \int_a^{a+\ell} E_o e^{jks} ds = \frac{E_o e^{j(\omega t_a + k\ell/2)}}{jk} \left(e^{jk\ell/2} - e^{-jk\ell/2}\right) \qquad \text{(A.2.14)}$$

Defining $\theta \equiv k\ell/2$, and rearranging terms, we get

$$V = E_o \ell \, e^{j(\omega t + k\ell/2)} \frac{\sin\theta}{\theta} \qquad \text{(A.2.15)}$$

Note that ignoring the overall phase factor is equivalent to asserting that the phase of the field is such that it reaches its peak value at the point when the particle is at the center of the accelerating gap (i.e. setting $t_a = -\ell/2v$).

The $E_o \ell$ term in Eq. A.2.15 is just what we would get if the field were not time-varying, i.e., apart from a phase factor, it is V_o. Hence, from Eq. A.2.13 we get the result that, for a uniform field in the s direction,

$$\boxed{T = \frac{\sin\theta}{\theta}} \qquad \text{(A.2.16)}$$

For most devices that employ nearly uniform longitudinal fields, it is common to assume that, unless stated otherwise, the transit time factor is given by Eq. A.2.16. For devices such as striplines (see Sect.) with short field gaps, T for each gap is approximately unity; for devices such as accelerating rf cavities, where the accelerating gap is a non-negligible fraction of the wavelength, T may be on the order of 0.5.

c. Integrals of Phasor Products; the Reciprocity Theorem

The reciprocity theorem as applied to kicker/pickup behavior took the form

$$V_B = -\frac{Z_c}{2V_K} \int_{vol} \mathbf{E}_K \cdot \mathbf{J}_B \, d\,vol. \qquad (1.2)$$

and it was noted that, unlike the integral in Eq. A.2.9, this one was to be evaluated at a *fixed time*. It was further noted that $\mathbf{J_B}$ was a sinusoidal wave of beam current, i.e. it is a term of the form $\mathbf{J}(x,y)\, e^{j(\omega t \pm ks)}$, the sign, as previously noted, depending on the direction of beam motion.

Two parenthetical notes: Although *all* the above integrals in Section 3 of this Appendix are for the frequency domain, this latter point did not arise in connection with the others; despite the fact that all but the one in Eq. A.2.12 related the time and position by the particle trajectory, none of them involved a beam-current term. Also, as we have seen from Sect. 3 in the main text, an actual beam contains not just a single wave of this form but is actually represented by a superposition of such waves.

Since the integral is to be evaluated at fixed time, the first term in the exponential assumes the role of (arbitrary) phase factor, to be treated in the same fashion as in the previously discussed integrals, and Eq. 1.2 takes the form

$$V_B = -\frac{Z_c}{2V_K}\int_{\substack{\text{beam}\\ \text{path}}} ds \int_{\substack{\text{beam}\\ \text{area}}} dxdy\, \mathbf{E}_K \cdot \mathbf{J}_B e^{-jks} \qquad \text{(A.2.17)}$$

If we assume that $\mathbf{E_K}$ does not vary over the beam cross section and make use of the fact that $\mathbf{J_B}$, and hence $\mathbf{I_B}$, define the s direction, we can integrate over the beam area and rewrite Eq. A.2.17 in the form

$$V_B = -\frac{Z_c}{2V_K}\int_{\substack{\text{beam}\\ \text{path}}} \mathbf{E_K} \cdot \mathbf{ds}\; e^{-jks} \qquad \text{(A.2.18)}$$

The form of the integral is strikingly similar to that of Eq. A.2.2. As in that equation, $k_B = \omega/v$, the beam wave number. However, not only is the origin of the exponential different (it results from the wave nature of the beam, rather than the frequency dependence of the field), but it has the opposite sign. (The physical import of this sign change is discussed in Sect. 4). Finally, as with Eq. A.2.10, we have made no assumptions about the *s*-dependence of $\mathbf{E_K}$, and the discussion in the paragraph immediately following that equation is equally applicable to Eq. A.2.18.

REFERENCES

1. R. Littauer, "Beam Instrumentation," in *Physics of High Energy Particle Accelerators*, ed. M. Month, AIP Conf. Proc. **105**, 869 (1983).

2. J. Borer and R. Jung, "Diagnostics," CERN/LEP-BI/84-14 (October 1984).

3. R.H. Siemann, "Bunched Beam Diagnostics," in *Physics of Accelerators*, eds. M. Month and M. Dienes, AIP Conf. Proc. **184**, 430 (1989).

4. P Strehl, "Beam Diagnostics," in *CERN Accelerator School, Second General Accelerator Physics Course*, ed. S. Turner, CERN Report **87-10**, 99 (1987).

5. H. Koziol, "Beam Diagnostics," in *CERN Accelerator School, Third General Accelerator Physics Course*, ed. S. Turner, CERN Report **89-05**, 63 (1989).

6. *Accelerator Instumentation*, eds. E.R.Beadle and V.J. Castillo, AIP Conf. Proc. **212**, (1990).

7. *Accelerator Instumentation*, ed. E.S. McCrory, AIP Conf. Proc. **229**, (1991).

8. J. Bisognano and C. Leemann, "Stochastic Cooling," in *Physics of High Energy Particle Accelerators*, eds. R. Carrigan, F. Huson, and M. Month, AIP Conf. Proc. **87**, 626 *et seq* (1982).

9. A.V. Tollestrup and G. Dugan, "Elementary Stochastic Cooling," in *Physics of High Energy Particle Accelerators*, ed. M. Month, AIP Conf. Proc. **105**, 1006 *et seq.* (1983).

10. G. Lambertson, "Dynamic Devices–Pickups and Kickers," in *Physics of Accelerators*, eds. M. Month and M. Dienes, AIP Conf. Proc. **153**, 1414 (1987).

11. G. Lambertson, "Electromagnetic Detectors," in *Frontiers of Particle Beams*, eds. M. Month and S. Turner, Springer-Verlag Lecture Notes in Physics **343**, 380 (1989).

12. R. E. Colin, *Foundations for Microwave Engineering*, pp. 56-59, McGraw-Hill, , New York, N.Y., (1966).

13. W.R. Smythe, *Static and Dynamic Electricity*, pp. 34-35, McGraw-Hill, , New York, N.Y., (1950)

14. W.K.H. Panofsky and W.A. Wenzel, Rev. Sci. Instr. **27**, 967 (1956).

15. S Chattopadhyay, "Some Fundamental Aspects of Fluctuations and Coherence in Charged-Particle Beams in Storage Rings," in *Physics of High Energy Particle Accelerators*, ed. M. Month, AIP Conf. Proc. **127**, 467 (1985).

16. D.A. Goldberg and G.R. Lambertson, "Successful Observation of Schottky Signals at the Tevatron Collider," Particle Accelerators **80**, 1 (1990).

17. D.A. Goldberg, W. Barry, G.R. Lambertson, and F. Voelker, "A High-Frequency Schottky Detector for Use in the Tevatron," in Proc. 1987 IEEE Particle Accelerator Conf., I.E.E.E. Catalog No. **87CH2387-9**, 547 (1987).

18. Q. Kerns, *et al.*, "Tuned Beam Position Detector for the Fermilab Switchyard," in Proc. 1987 IEEE Particle Accelerator Conf., I.E.E.E. Catalog No. **87CH2387-9**, 661 (1987).

19. T.P.R. Linnecar, "The High Frequency Longitudinal and Transverse Pick-ups in the CERN SPS Accelerator," IEEE Trans. Nucl. Sci. **NS-26**, 3409 (June, 1979).

20. R. Shafer, "Characteristics of Directional Coupler Beam Position nonitors," IEEE Trans. Nucl. Sci. **NS-32**, 1933 (October, 1985).

21. D.A. Goldberg, G.R. Lambertson, F. Voelker, and L. Shalz, "Measurement of Frequency Response of LBL Stochastic Cooling Arrays for TEV-I Storage Rings," IEEE Trans. Nucl. Sci. **NS-32**, 1857 (October, 1985).

22. G.R. Lambertson, "Feeadback to Suppress Beam Instabilities in Future Proton Rings," IEEE Trans. Nucl. Sci. **NS-32**, 2168 (October, 1985).

23. G.R. Lambertson, "The Helix as a Beam Electrode," Lawrence Berkeley Laboratory, internal report BECON-60 (August, 1985).

24. H. Yonehara, et al., INS-NUMA-49 (1983).

25. G.R. Lambertson, et al., "Experiments on Stochastic Cooling of 200 MeV Protons," IEEE trans. Nucl. Sci. **NS-28**, 2471 (June, 1981).

26. G. Lambertson, K. J. Kim, and F. Voelker, "The Slotted Coax as a Beam Electrode, IEEE Trans. Nucl. Sci. **NS-30**, 2158 (August, 1983).

27. D. Boussard and G. DiMassa, "High Frequency Slow Wave Pickups," CERN-SPS/86-4(ARF), (February, 1986).